



Weill Cornell Medical College

Institute for Computational Biomedicine



ChIP-seq and Hi-C

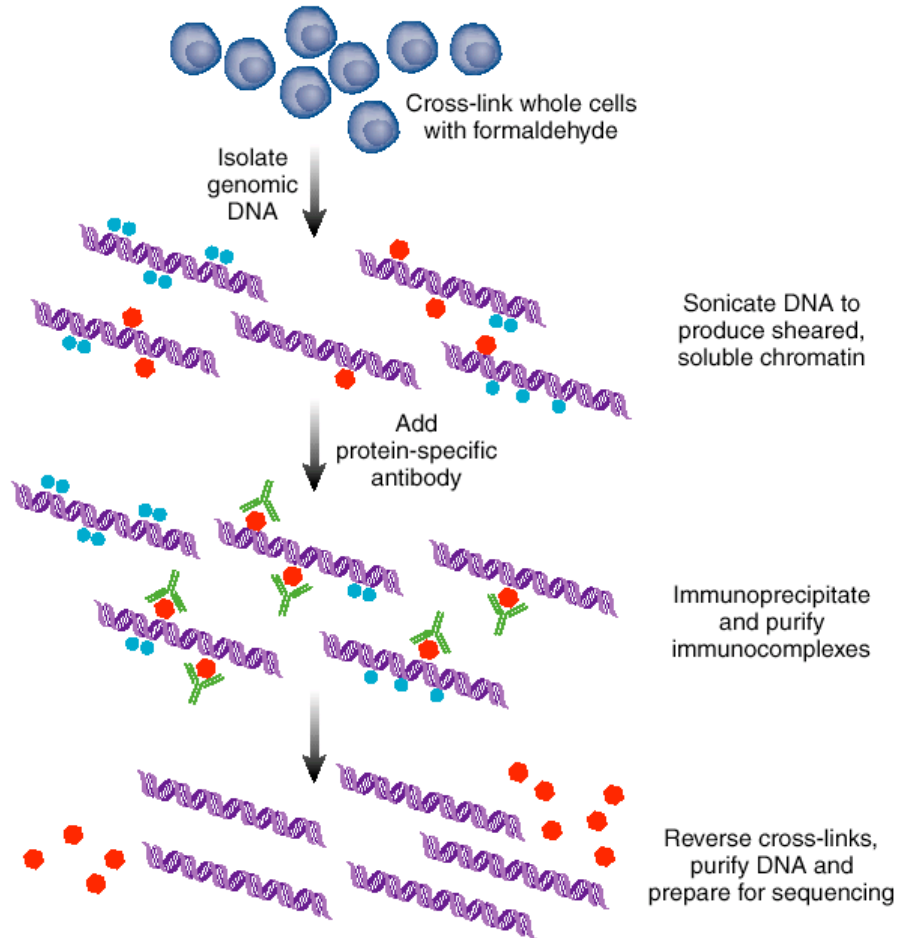
Olivier Elemento, PhD

Laboratory of Cancer Systems Biology

Plan

1. ChIP-seq
2. A few interesting ChIP-seq papers
3. Quality Control of ChIP-seq data
4. ChIP-seq Peak detection
5. Peak Analysis and Interpretation
6. Mapping chromatin interactions using Hi-C

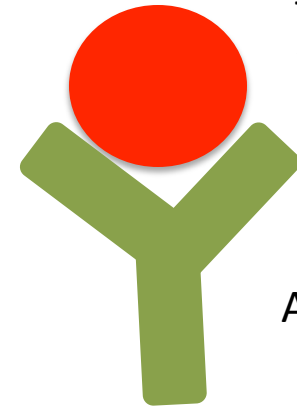
ChIP-seq



Sonicate DNA to produce sheared, soluble chromatin

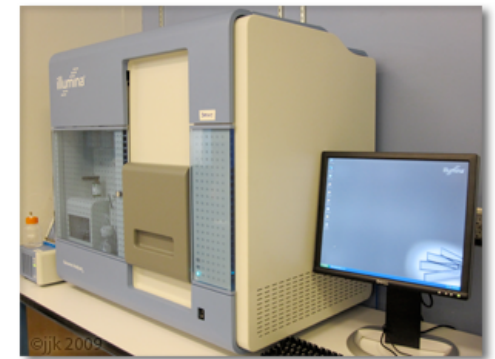
Immunoprecipitate and purify immunocomplexes

Reverse cross-links, purify DNA and prepare for sequencing



Transcription factor of interest (or histone modification)

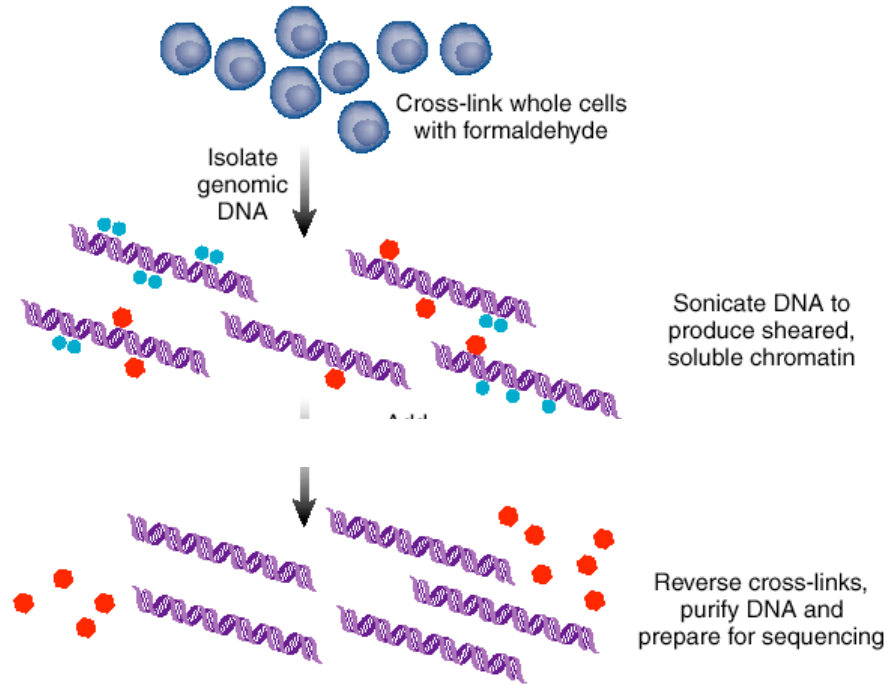
Antibody



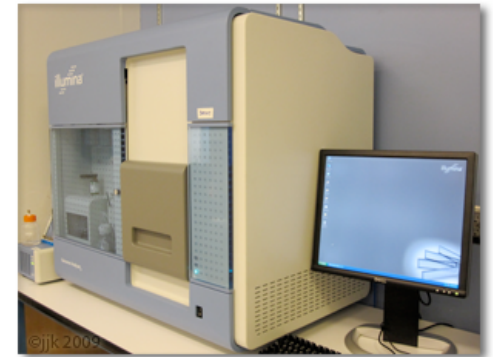
Illumina

Katle Rit

Control: input DNA



Katie Ris



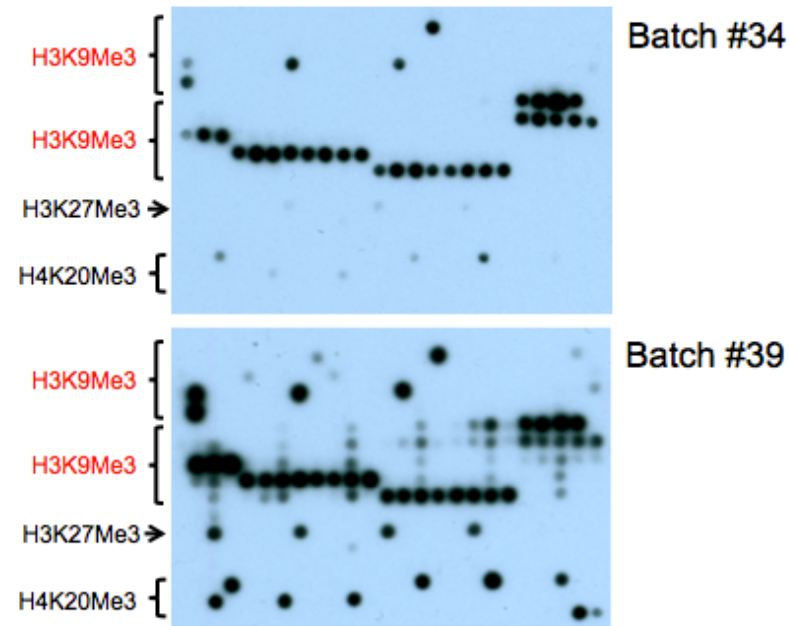
Illumina

Can use IgG as additional control

ChIP-seq methodology

- Identify ChIP-grade antibody, determine specificity (Western, histone peptide array)
- Optimize conditions using single-locus ChIP-PCR (positive and negative controls)
- Sequence ChIP product using 1 Illumina lane per sample (no TruSeq ChIP-seq), single end
- Sequence input/IgG as control

Abcam H3K9Me3 rabbit polyclonal (ab8898)



Assessing the specificity of a commercial H3K9m3 antibody using histone peptide arrays, K. Bunting & B. Swed, WCMC

First ChIP-seq paper

Genome-Wide Mapping of in Vivo Protein-DNA Interactions

David S. Johnson,^{1*} Ali Mortazavi,^{2*} Richard M. Myers,^{1†} Barbara Wold^{2,3†}

In vivo protein-DNA interactions connect each transcription factor with its direct targets to form a gene network scaffold. To map these protein-DNA interactions comprehensively across entire mammalian genomes, we developed a large-scale chromatin immunoprecipitation assay (ChIPSeq) based on direct ultrahigh-throughput DNA sequencing. This sequence census method was then used to map in vivo binding of the neuron-restrictive silencer factor (NRSF; also known as REST, for repressor element-1 silencing transcription factor) to 1946 locations in the human genome. The data display sharp resolution of binding position [± 50 base pairs (bp)], which facilitated our finding motifs and allowed us to identify noncanonical NRSF-binding motifs. These ChIPSeq data also have high sensitivity and specificity [ROC (receiver operator characteristic) area ≥ 0.96] and statistical confidence ($P < 10^{-4}$), properties that were important for inferring new candidate interactions. These include key transcription factors in the gene network that regulates pancreatic islet cell development.

Although much is known about transcription factor binding and action at specific genes, far less is known about the composition and function of entire factor-DNA

chromosome can be detected by chromatin immunoprecipitation (ChIP) (1). In ChIP experiments, an immune reagent specific for a DNA binding factor is used to enrich target DNA

putational discovery of binding motifs feasible, this dictates the quality of regulatory site annotation relative to other gene anatomy landmarks, such as transcription start sites, enhancers, introns and exons, and conserved noncoding features (2). Finally, if high-quality protein-DNA interactome measurements can be performed routinely and at reasonable cost, it will open the way to detailed studies of interactome dynamics in response to specific signaling stimuli or genetic mutations. To address these issues, we turned to ultrahigh-throughput DNA sequencing to gain sampling power and applied size selection on immuno-enriched DNA to enhance positional resolution.

The ChIPSeq assay shown here differs from other large-scale ChIP methods such as ChIPArray, also called ChIPchip (1); ChIPSAGE (SACO) (3); or ChIPPet (4) in design, data produced, and cost. The design is simple (Fig. 1A) and, unlike SACO or ChIPPet, it involves no plasmid library construction. Unlike microarray assays, the vast majority of single-copy sites in the genome is accessible for ChIPSeq assay (5), rather than a subset selected to be array features.

Epigenetic modifications at enhancer regions

doi:10.1038/nature07829

nature

LETTERS

Histone modifications at human enhancers reflect global cell-type-specific gene expression

Nathaniel D. Heintzman^{1,2*}, Gary C. Hon^{1,3*}, R. David Hawkins^{1*}, Pouya Kheradpour⁵, Alexander Stark^{5,6}, Lindsey F. Harp¹, Zhen Ye¹, Leonard K. Lee¹, Rhona K. Stuart¹, Christina W. Ching¹, Keith A. Ching¹, Jessica E. Antosiewicz-Bourget⁷, Hui Liu⁸, Xinmin Zhang⁸, Roland D. Green⁸, Victor V. Lobanenko⁹, Ron Stewart⁷, James A. Thomson^{7,10}, Gregory E. Crawford¹¹, Manolis Kellis^{5,6} & Bing Ren^{1,4}

The human body is composed of diverse cell types with distinct functions. Although it is known that lineage specification depends on cell-specific gene expression, which in turn is driven by promoters, enhancers, insulators and other *cis*-regulatory DNA sequences for each gene^{1–3}, the relative roles of these regulatory elements in this process are not clear. We have previously developed a chromatin-immunoprecipitation-based microarray method (ChIP-chip) to locate promoters, enhancers and insulators in the human genome^{4–6}. Here we use the same approach to

Next, we identified putative insulators in the ENCODE regions for these cell types based on CTCF binding, because mammalian insulators are generally understood to require CTCF to block promoter–enhancer interactions⁵. We observed nearly identical CTCF occupancy (Supplementary Table 1 and Supplementary Fig. 1e) and highly correlated CTCF enrichment patterns across all five cell types (Supplementary Fig. 1b), providing experimental support for the mostly cell-type-invariant function of CTCF as suggested by DNase hypersensitivity mapping results⁸.

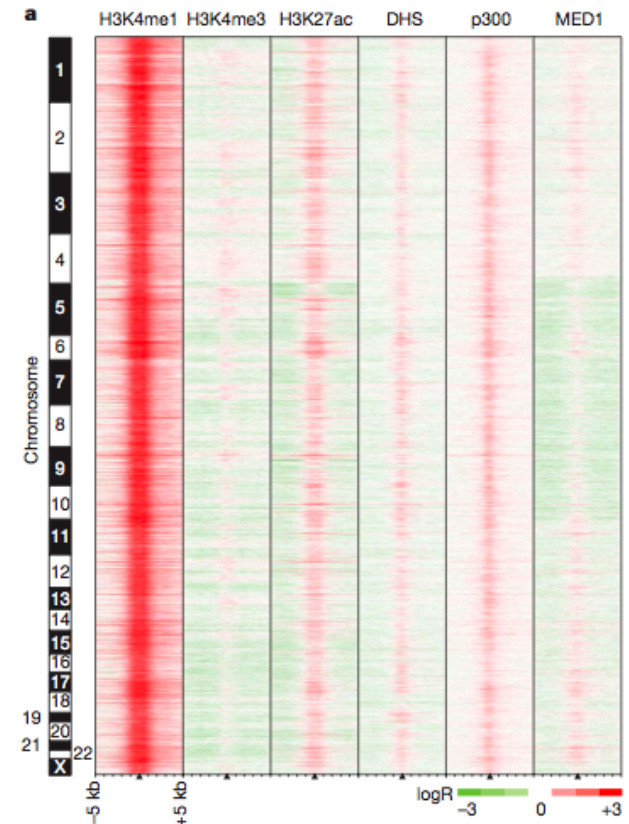


Figure 2 | Genome-wide enhancer predictions in human cells. a, We predict 36,589 enhancers in HeLa cells on the basis of chromatin signatures for H3K4me1 and H3K4me3 as determined by ChIP-chip using genome-wide tiling microarrays and condensed enhancer microarrays (see Supplementary Information). Enhancer predictions are located at the centre of 10-kb

Chromatin states

ARTICLE

doi:10.1038/nature09906

Mapping and analysis of chromatin state dynamics in nine human cell types

Jason Ernst^{1,2}, Pouya Kheradpour^{1,2}, Tarjei S. Mikkelsen¹, Noam Shores¹, Lucas D. Ward^{1,2}, Charles B. Epstein¹, Xiaolan Zhang¹, Li Wang¹, Robbyn Issner¹, Michael Coyne¹, Manching Ku^{1,3,4}, Timothy Durham¹, Manolis Kellis^{1,2*} & Bradley E. Bernstein^{1,3,4*}

Chromatin profiling has emerged as a powerful means of genome annotation and detection of regulatory activity. The approach is especially well suited to the characterization of non-coding portions of the genome, which critically contribute to cellular phenotypes yet remain largely uncharted. Here we map nine chromatin marks across nine cell types to systematically characterize regulatory elements, their cell-type specificities and their functional interactions.

Focusing on cell-type-specific patterns of chromatin state, gene expression, regulatory motif profiles to link enhancers to putative target genes. The resulting annotations are used in genome-wide association studies. Top-predicted enhancer elements specifically associated with a predicted regulator, thus suggesting a role in deciphering *cis*-regulatory connections.

A major challenge in biology is understanding how a cell can give rise to an organism comprising hundreds of different cell types. Much emphasis has been placed on the application of tools to study interacting cellular components¹. In recent years, molecular biology has exploited dynamic gene expression patterns to identify functional modules, pathways and networks². Yet *cis*-

b

State	CTCF	H3K27me3	H3K36me3	H4K20me1	H3K4me1	H3K4me2	H3K4me3	H3K27ac	H3K9ac	WCE
1	16	2	2	6	17	93	99	96	98	2
2	12	2	6	9	53	94	95	14	44	1
3	13	72	0	9	46	78	49	1	10	1
4	11	1	15	11	96	99	75	97	86	4
5	5	0	10	3	86	57	5	84	25	1
6	7	1	1	3	58	75	8	6	5	1
7	2	1	2	1	56	3	0	6	2	1
8	92	2	1	3	6	3	0	0	1	1
9	5	0	43	43	37	11	2	9	4	1
10	1	0	47	3	0	0	0	0	0	1
11	0	0	3	2	0	0	0	0	0	0
12	1	27	0	2	0	0	0	0	0	0
13	0	0	0	0	0	0	0	0	0	0
14	22	28	19	41	6	5	26	5	13	37
15	85	85	91	88	76	77	91	73	85	78

Chromatin mark observation frequency (%)

c

Chromatin states	Coverage										Median length (kb)	±2 kb TSS (%)	Functional enrichments (fold)					Transcript (NHLF)	Nuclear lamina (NHLF)	Candidate state annotation
	Median	H1	ES	GM	Conserved non-exon	DNase (K562)	c-Myc (K562)	NF-κB (GM12878)	Transcript	Nuclear lamina										
1	0.6	0.5	1.2	1.0	83	3.8	23.3	82.0	40.7	0.2	0.15	Active promoter								
2	0.5	1.2	1.3	0.4	58	2.8	15.3	12.6	5.8	0.6	0.30	Weak promoter								
3	0.2	4.0	1.0	0.6	49	4.3	10.8	3.1	1.0	0.4	0.68	Inactive/poised promoter								
4	0.7	0.1	1.1	0.6	23	2.7	23.1	31.8	49.0	1.3	0.05	Strong enhancer								
5	1.2	0.2	0.7	0.6	3	1.8	13.6	6.3	15.8	1.4	0.10	Strong enhancer								
6	0.9	1.3	1.0	0.2	17	2.4	11.9	5.7	7.0	1.1	0.31	Weak/poised enhancer								
7	1.9	1.2	1.1	0.4	4	1.5	5.1	0.6	2.4	1.3	0.20	Weak/poised enhancer								
8	0.5	1.4	1.0	0.4	3	1.5	12.8	2.5	1.2	1.1	0.61	Insulator								
9	0.7	1.3	1.0	0.8	4	1.1	4.5	0.7	0.8	2.4	0.02	Transcriptional transition								
10	4.3	0.6	1.2	3.0	1	0.9	0.3	0.0	0.0	2.5	0.11	Transcriptional elongation								
11	12.5	1.3	0.8	2.6	2	0.9	0.3	0.0	0.1	1.9	0.24	Weak transcribed								
12	4.1	0.3	0.7	2.8	5	1.4	0.3	0.0	0.1	0.8	0.63	Polycomb repressed								
13	71.4	1.0	1.0	10.0	1	0.9	0.1	0.0	0.0	0.7	1.30	Heterochrom; low signal								
14	0.1	0.9	1.2	0.6	3	0.4	1.9	0.3	0.2	0.4	1.44	Repetitive/CNV								
15	0.1	0.9	1.0	0.2	1	0.2	5.9	9.5	7.4	0.4	1.30	Repetitive/CNV								

Chromatin mark observation frequency (%) (%) (fold) (kb) (%) Functional enrichments (fold)

Differential oestrogen receptor binding is associated with clinical outcome in breast cancer

Caryn S. Ross-Innes¹, Rory Stark¹, Andrew E. Teschendorff², Kelly A. Holmes¹, H. Raza Ali^{1,8}, Mark J. Dunning¹, Gordon D. Brown¹, Ondrej Gojis^{3,4,5}, Ian O. Ellis⁶, Andrew R. Green⁶, Simak Ali³, Suet-Feung Chan^{1,7}, Carlos Caldas^{1,7,8,9} & Jason S. Carroll^{1,7}

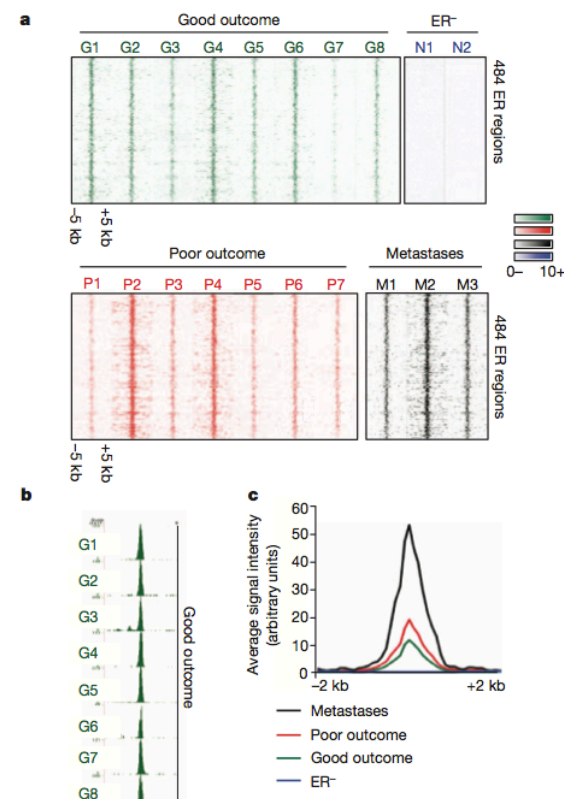
Oestrogen receptor- α (ER) is the defining and driving transcription factor in the majority of breast cancers and its target genes dictate cell growth and endocrine response, yet genomic understanding of ER function has been restricted to model systems^{1–3}. Here we map genome-wide ER-binding events, by chromatin immunoprecipitation followed by high-throughput sequencing (ChIP-seq), in primary breast cancers from patients with different clinical outcomes and in distant ER-positive metastases. We find that drug-resistant cancers still recruit ER to the chromatin, but that ER binding is a dynamic process, with the acquisition of unique ER-binding regions in tumours from patients that are likely to relapse. The acquired ER regulatory regions associated with poor clinical outcome observed in primary tumours reveal gene signatures that predict clinical outcome in ER-positive disease exclusively. We find that the differential ER-binding programme observed in tumours from patients with poor outcome is not due to the selection of a rare subpopulation of cells, but is due to the FOXA1-mediated reprogramming of ER binding on a rapid timescale. The parallel redistribution of ER and FOXA1 binding events

in breast cancer (Supplementary Fig. 1). As a control, we analysed metastatic locations and samples that were ER⁻ (ER- α negative), ER- β .

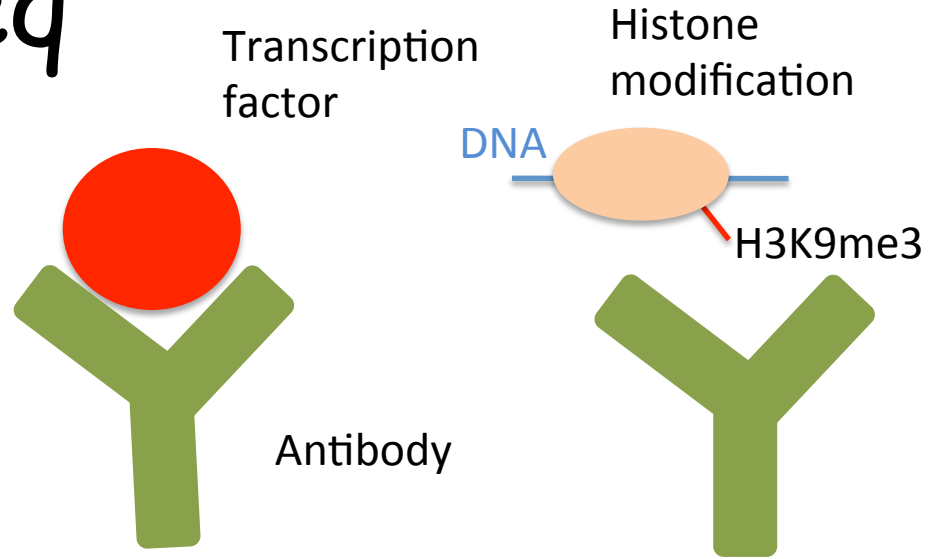
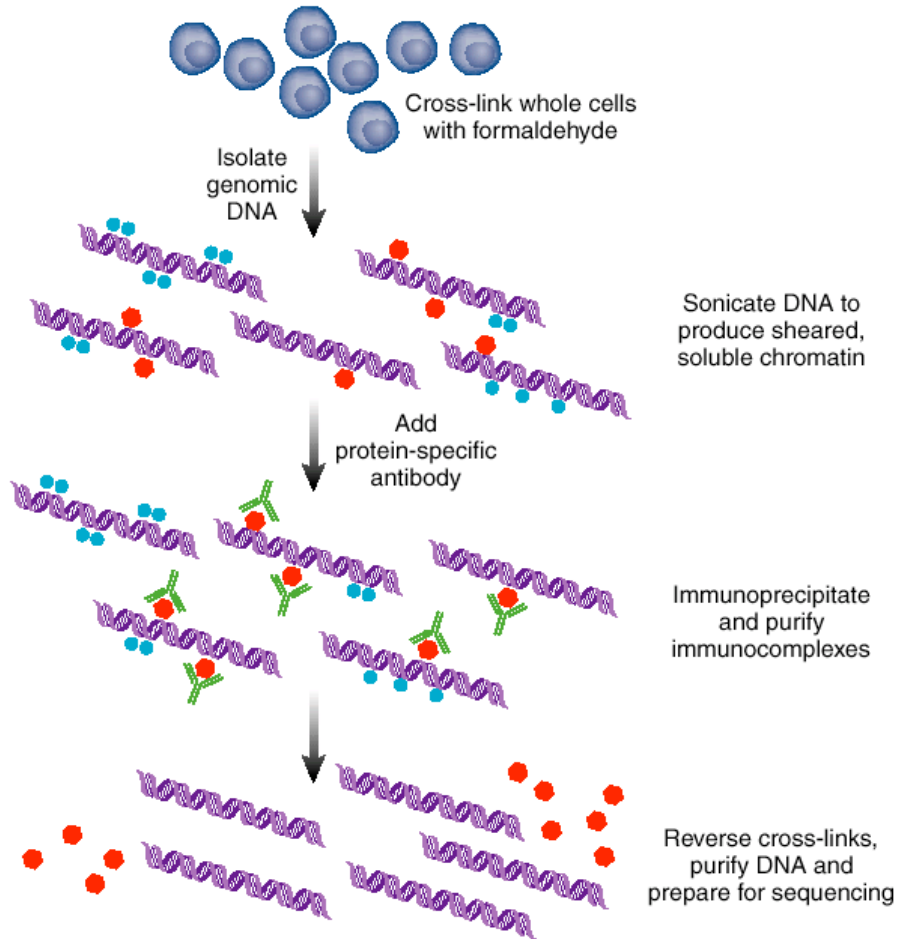
ER ChIP-seq was conducted using two different algorithms, ebi.ac.uk/~swilder/SWEMBL/ number of sequencing reads as is shown in Supplementary Fig. 2, but total peak intensities differed. Three tumours ChIP-seq was conducted on the concordance when comparing ($R^2 = 0.954$) suggesting that they mutually influence the ER-binding programme (Supplementary Fig. 3).

We initially assessed whether

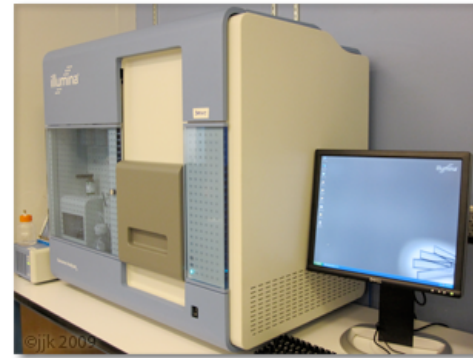
RESEARCH LETTER



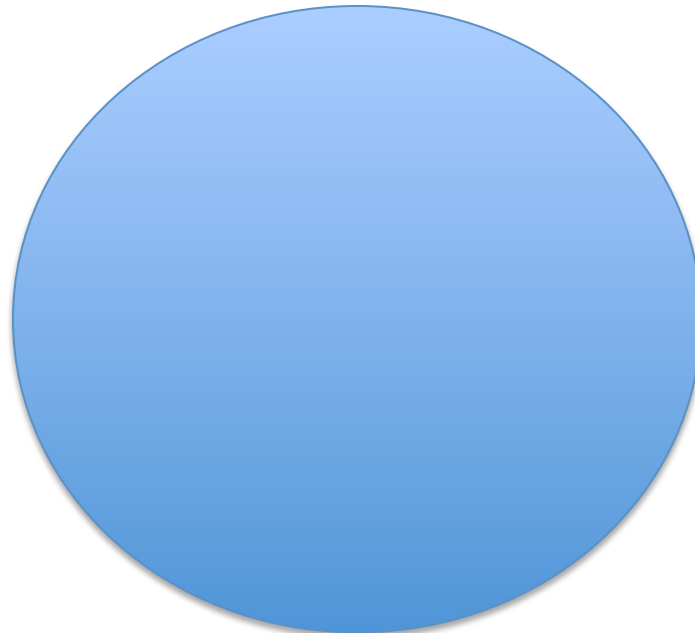
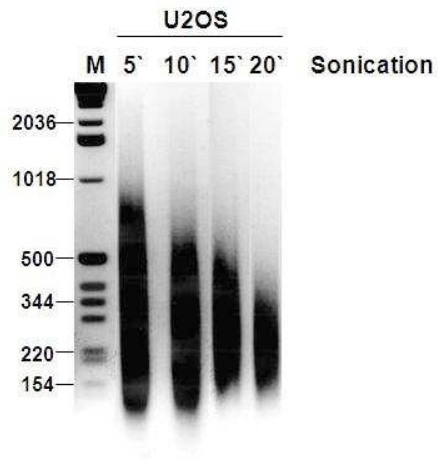
ChIP-seq



Katje Rits



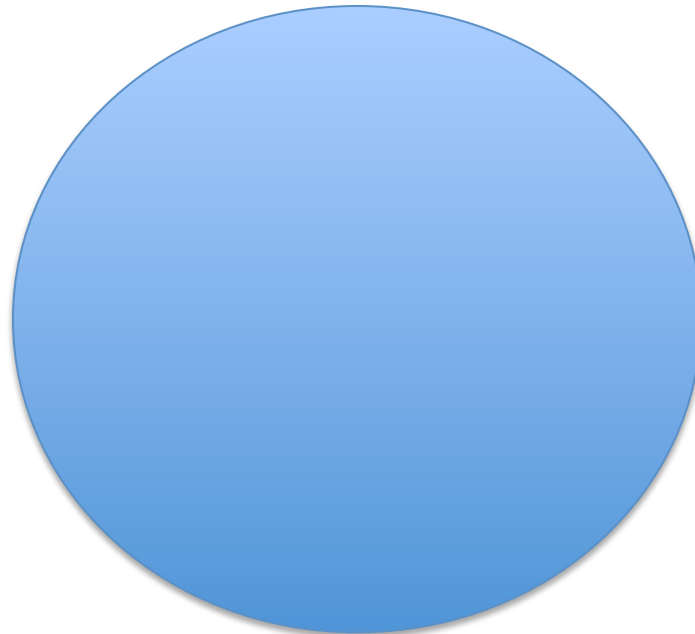
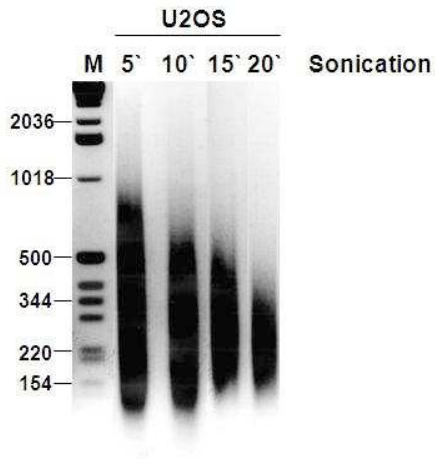
Illumina



ACCAATAACCGAGGCTCATGCTAAGGCGTTAGCCACAGATG**GAAGTCCGA**CGGCTTGATCCAGAATGGTGTGTGGATTGCCTTGGAAGTATTAGTGAATTC
TGGTTATTGGCTCCGAGTACGATTCCGCAATCGGTGTCTAC**CTTCAGGCT**GCCGAACTAGGTCTTACCACACACCTAACGGAACCTTGACTAATCACTTAAG



Average length ~ 170bp



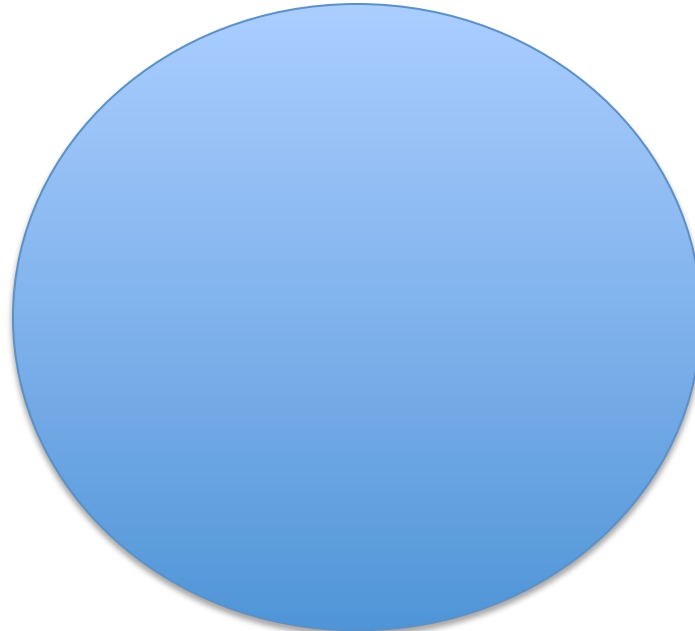
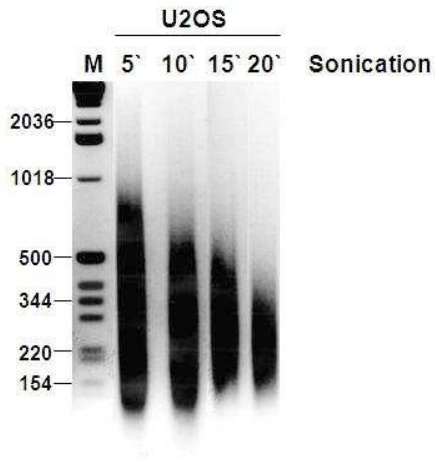
40-100bp



ACCAATAACCGAGGCTCATGCTAAGGCGTTAGCCACAGATG**GAAGTCCGA**CGGCTTGATCCAGAATGGTGTGTGGATTGCCTTGGAAGTATTAGTGAATTC
 TGGTTATTGGCTCCGAGTACGATTCCGCAATCGGTGTCTAC**CTTCAGGCT**GCCGAACTAGGTCTTACCACACACCTAACGGAACCTTGACTAATCACTTAAG



Average length ~ 170bp



40-100bp



ACCAATAACCGAGGCTCATGCTAAGGCGTTAGCCACAGATGGAAGTCCGACGGCTTGATCCAGAATGGTGTGTGGATTGCCTTGGAACTGATTAGTGAATTC
 TGGTTATTGGCTCCGAGTACGATTCCGCAATCGGTGTCTACCTTCAGGCTGCCGAACTAGGTCTTACCACACACCTAACGGAACCTTGACTAATCACTTAAG



Average length ~ 170bp

BWA tutorial (for aligning single end reads to genome)

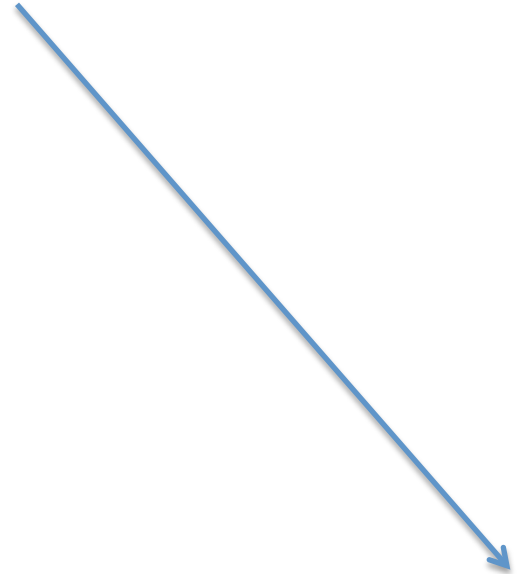
- Get genome, e.g., from UCSC
 - <http://hgdownload.cse.ucsc.edu/goldenPath/hg19/bigZips/chromFa.tar.gz>
- Combine into 1 file
 - `tar zvfx chromFa.tar.gz`
 - `cat *.fa > wg.fa`
- Indexing the genome
 - `bwa index -p hg19bwaidx -a bwtsv wg.fa`
- **Align CHIP reads to reference genome**
 - `bwa aln -t 4 hg19bwaidx s_3_sequence.txt.gz > s_3_sequence.txt.bwa`
- Convert to SAM format
 - `bwa samse hg19bwaidx s_3_sequence.txt.bwa s_3_sequence.txt.gz > s_3_sequence.txt.sam`
- **Align input reads to same reference genome**
 - `bwa aln -t 4 hg19bwaidx s_4_sequence.txt.gz > s_4_sequence.txt.bwa`
- Convert to SAM format
 - `bwa samse hg19bwaidx s_4_sequence.txt.bwa s_4_sequence.txt.gz > s_4_sequence.txt.sam`

Reads can map to multiple locations/chromosomes

Read 1



Read 2



Reference Human Genome (hg19)

Reads map to one strand or the other

Read 1



Read 2



hg18

SAM format

```
DH1608P1_0130:6:1103:10579:166379#TTAGGC 16 chr1 1249828 37 51M * 0 0
GGGCGTGACTCTGATCTCAGGCATCGTCTCCGCCGCGCTCCCGGACCCGCG eb`XXYbZdadee^ceV]X][ccTcc^ebeeece
eeeWbeeeeeeeceeeae XX:Z:NM_017871,32 NM:i:0 MD:Z:51

DH1608P1_0130:6:1102:3415:150915#TTAGGC 16 chr1 1249828 37 51M * 0 0
GGGCGGGACTCTGATCTCAGGCATCGTCTCCGCCGCGCTCCCGGACCCGCG BBBBBBBBBBBac]bbbceedaeddeZceee_a_\_eee
eeeedaeeee XX:Z:NM_017871,32 NM:i:1 MD:Z:5T45

DH1608P1_0130:6:1102:13118:62644#TTAGGC 16 chr1 1249828 37 51M * 0 0
GGGCGTGCCTCGGATCTCAGGCATCGTCTCCGCCGCGCTCCCGGACCCGCG BBBBBBBBBBBBBBBBBBBBB`XTbSa`cffegdggeccbe
effdegggg XX:Z:NM_017871,32 NM:i:2 MD:Z:7A3T39

DH1608P1_0130:6:1203:3012:157120#TTAGGC 16 chr1 1249826 25 51M * 0 0
AAGGCCGTGACTCTGATCTCAGCCCTCGTCTCCGCCGCGCTCCCGGACCCG BBBBBBBB^`QWZZ]UXYSZSTFRU]Z__SO[adcc[acdV
\`Y]YWY][_ XX:Z:NM_017871,34 NM:i:3 MD:Z:4G17G1A26

DH1608P1_0130:6:2206:4445:12756#TTAGGC 16 chr1 1246336 25 1M3487N50M * 0 0
CCAAAGGGTGTGACTCTGATCTCGGGCATCGTCTCCGCCGCGCTCCCGGAC BBBBBBBBBBBBBBBBBBBBBBB`YdddYdc\
cacaNdddddcdadeeee XX:Z:NM_017871,37 NM:i:3 MD:Z:2C5C14A27

DH1608P1_0130:6:2203:7903:43788#TTAGGC 16 chr1 1246336 37 1M3487N50M * 0 0
CCCAAGGGCGTGACTCTGATCTCAGGCATCGTCTCCGCCGCGCTCCCGGAC adbe[fbcbccb_cb^cb^c^edgeggggdf
ggefffgfbfgggegeg XX:Z:NM_017871,37 NM:i:0 MD:Z:51
```

CIGAR string, eg 5M3487N46M = 5bp-long block, 3487 insert, 46bp-long block

MD tag, e.g, MD:Z:4T46 = 5 matches, 1 mismatch (T in read), 46 matches

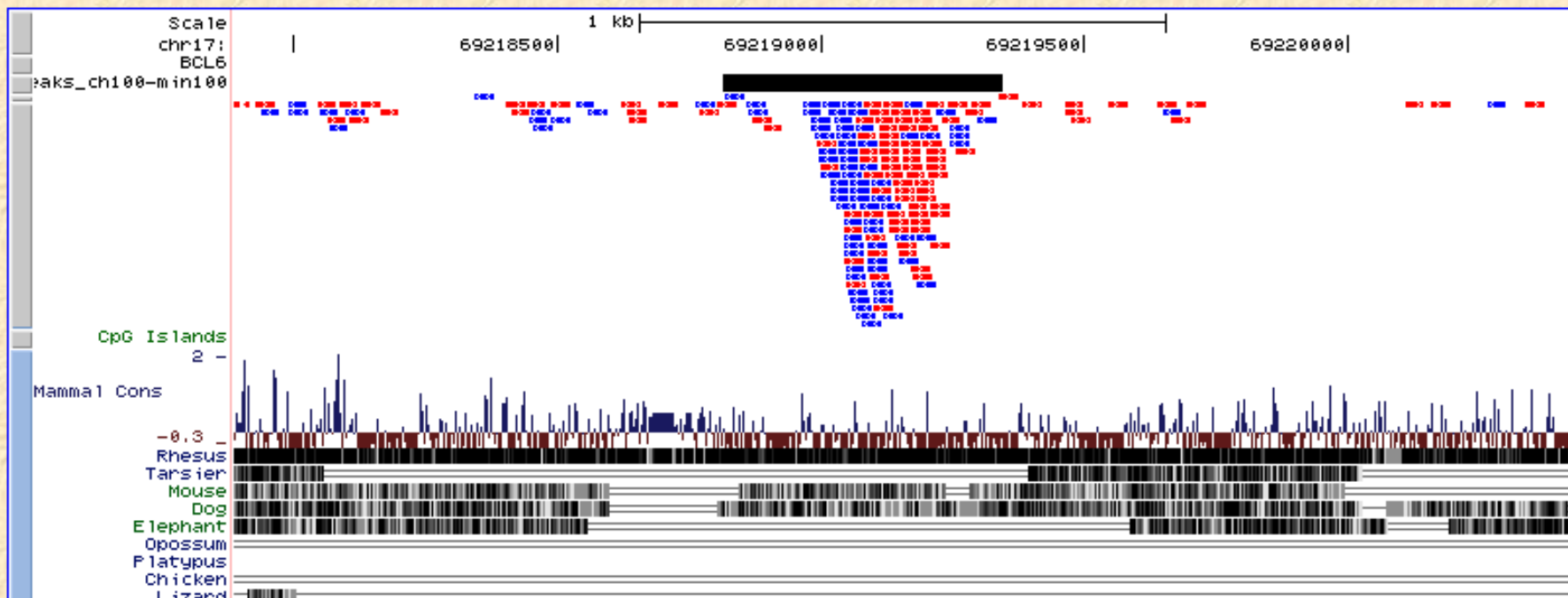
XT tag, e.g. XT:A:U = unique mapper; XT:A:R = more than 1 high-scoring matches

UCSC Genome Browser on Human Mar. 2006 Assembly (hg18)

move <<< << < > >> >>> zoom in 1.5x 3x 10x base zoom out 1.5x 3x 10x

position/search jump clear size 2,537 bp. configure

chr17 (q25.1) 13.3 p13.1 17p12 17p11.2 q11.2 17q12 17q22 24.3 5.1 q25.3



chr16:

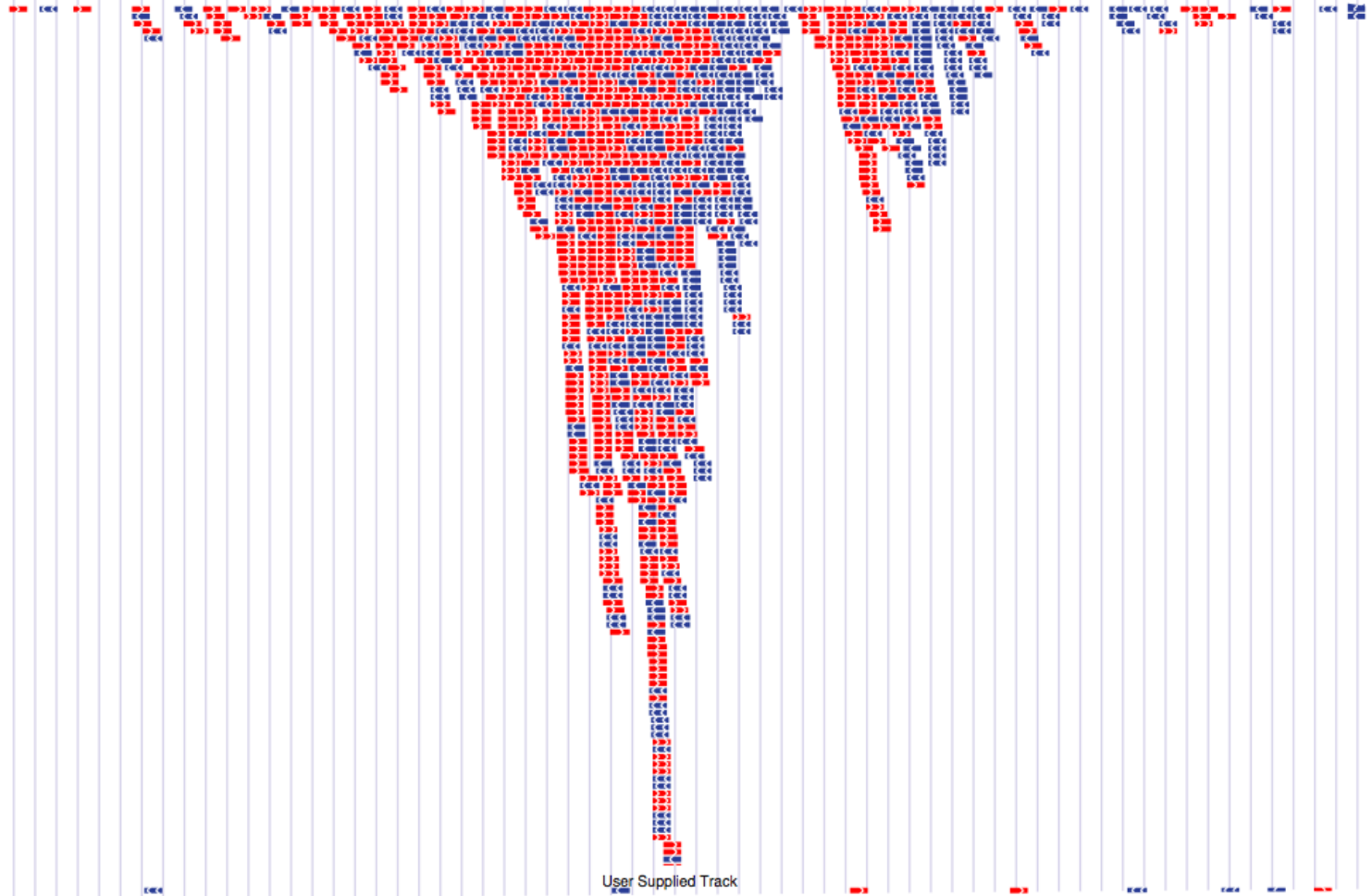
91930500 |

91931000 |

91931500 |

91932000 |

91932500 |



User Supplied Track

ChIP-seq peak calling

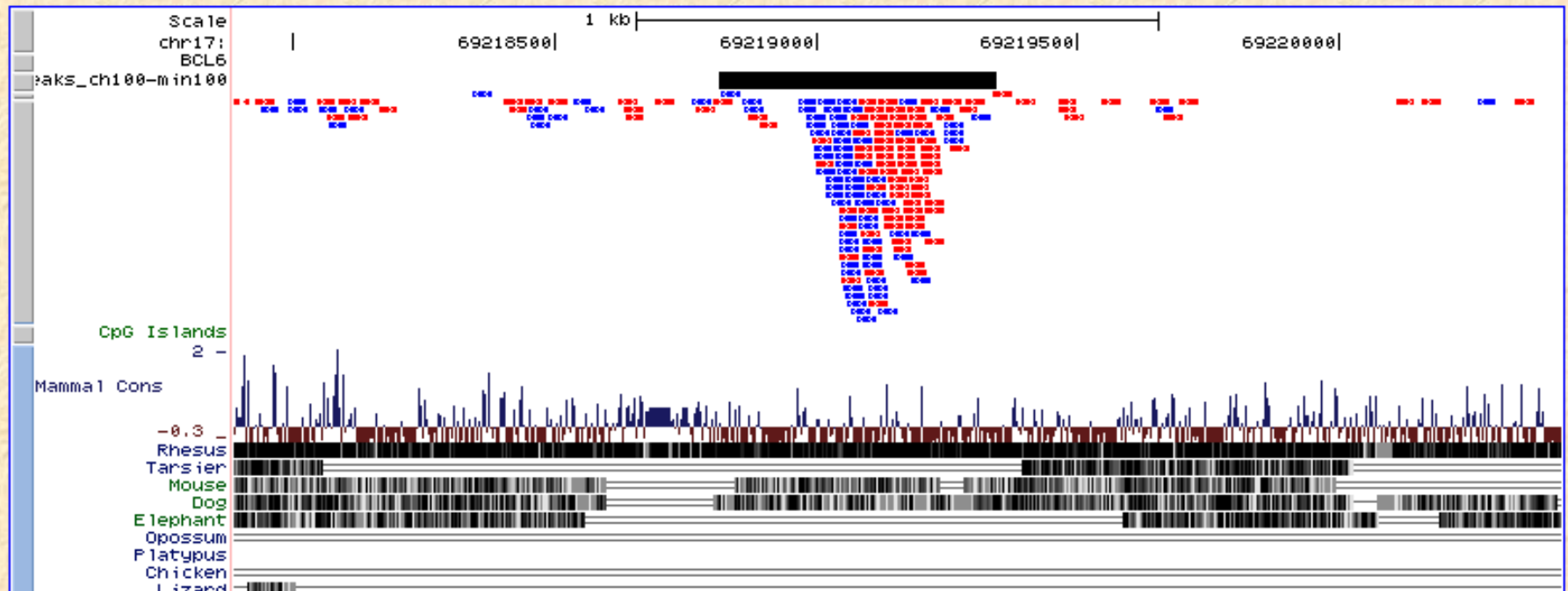
A nice peak

UCSC Genome Browser on Human Mar. 2006 Assembly (hg18)

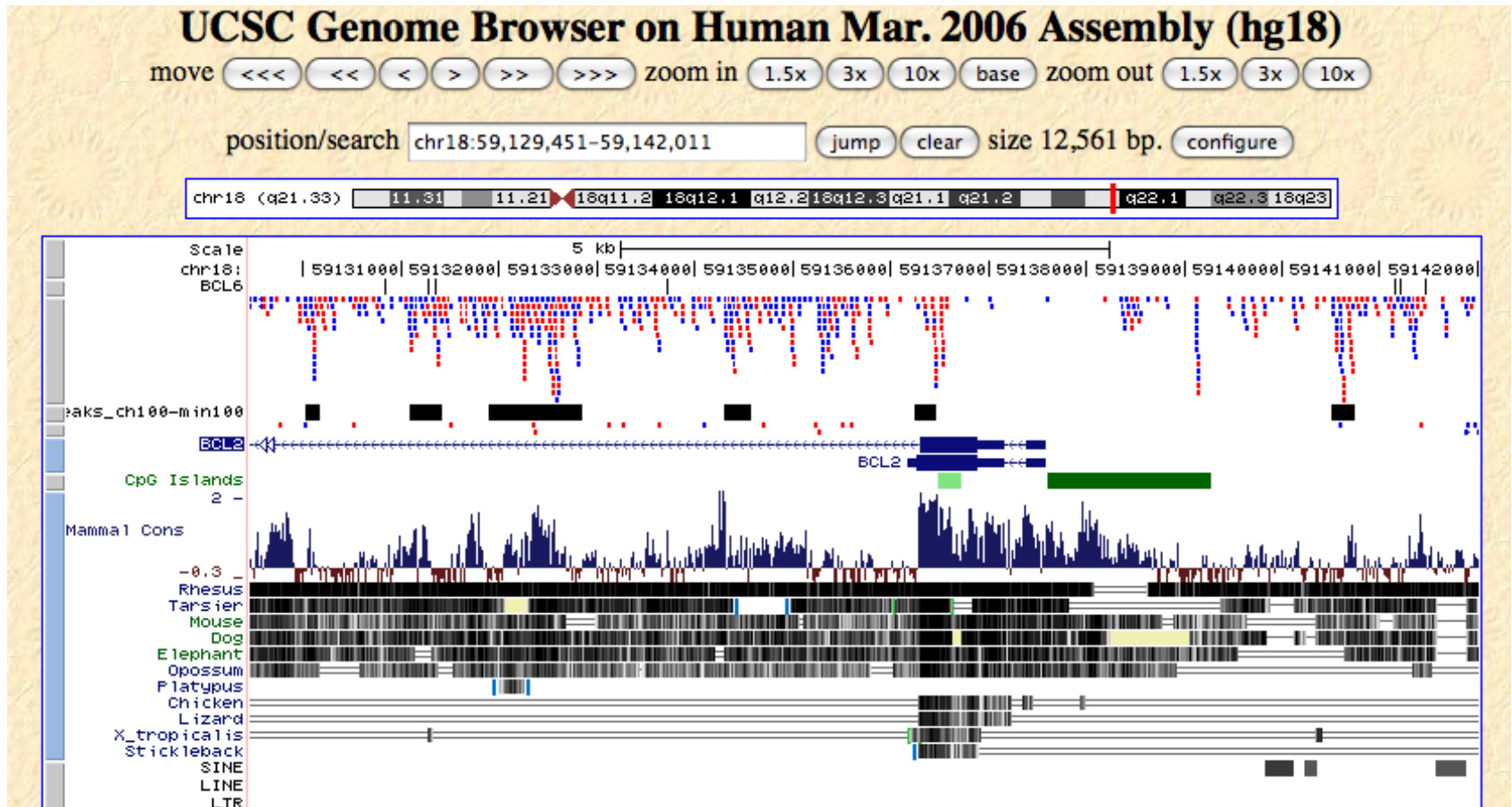
move <<<< << < > >> >>> zoom in 1.5x 3x 10x base zoom out 1.5x 3x 10x

position/search chr17:69,217,888-69,220,424 jump clear size 2,537 bp. configure

chr17 (q25.1) 13.3 p13.1 17p12 17p11.2 q11.2 17q12 17q22 24.3 5.1 q25.3



Not all peaks are nice



MACS

Open Access

Method

Model-based Analysis of ChIP-Seq (MACS)

Yong Zhang^{✉*}, Tao Liu^{✉*}, Clifford A Meyer^{*}, Jérôme Eeckhoute[†],
David S Johnson[‡], Bradley E Bernstein^{§¶}, Chad Nussbaum[¶],
Richard M Myers[∫], Myles Brown[†], Wei Li[#] and X Shirley Liu^{*}

Addresses: ^{*}Department of Biostatistics and Computational Biology, Dana-Farber Cancer Institute and Harvard School of Public Health, 44 Binney Street, Boston, MA 02115, USA. [†]Division of Molecular and Cellular Oncology, Department of Medical Oncology, Dana-Farber Cancer Institute and Department of Medicine, Brigham and Women's Hospital and Harvard Medical School, 44 Binney Street, Boston, MA 02115, USA. [‡]Gene Security Network, Inc., 2686 Middlefield Road, Redwood City, CA 94063, USA. [§]Molecular Pathology Unit and Center for Cancer Research, Massachusetts General Hospital and Department of Pathology, Harvard Medical School, 13th Street, Charlestown, MA 02129, USA. [¶]Broad Institute of Harvard and MIT, 7 Cambridge Center, Cambridge, MA, 02142, USA. [∫]Department of Genetics, Stanford University Medical Center, Stanford, CA 94305, USA. [#]Division of Biostatistics, Dan L Duncan Cancer Center, Department of Molecular and Cellular Biology, Baylor College of Medicine, One Baylor Plaza, Houston, TX 77030, USA.

✉ These authors contributed equally to this work.

Correspondence: Wei Li. Email: wli@bcm.edu. X Shirley Liu. Email: xshliu@jimmy.harvard.edu

Published: 17 September 2008

Genome Biology 2008, **9**:R137 (doi:10.1186/gb-2008-9-9-r137)

The electronic version of this article is the complete one and can be found online at <http://genomebiology.com/2008/9/9/R137>

Received: 4 August 2008

Revised: 3 September 2008

Accepted: 17 September 2008

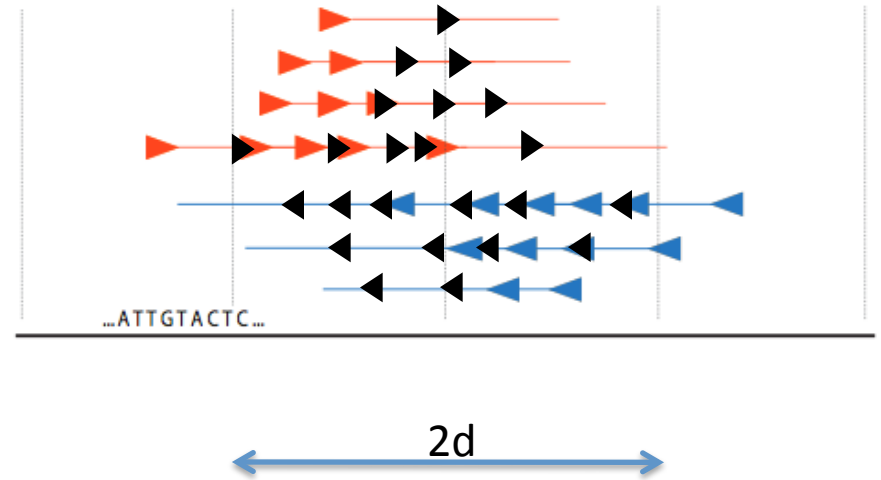
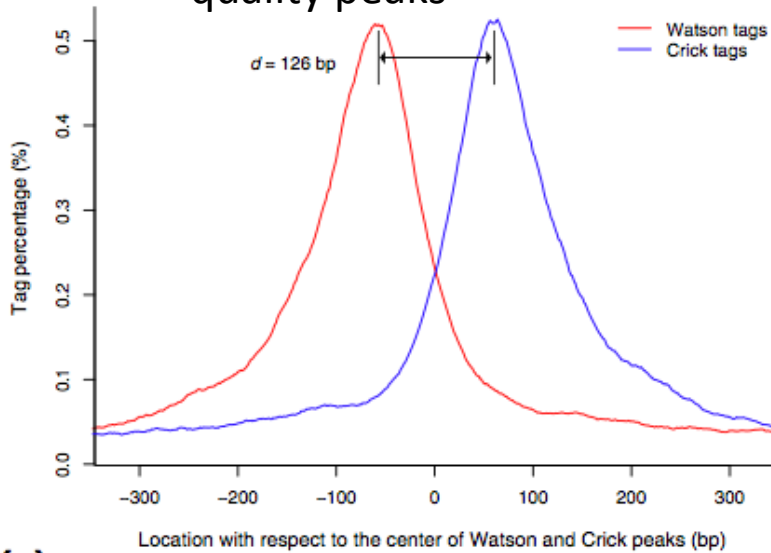
© 2008 Zhang *et al.*; licensee BioMed Central Ltd.

This is an open access article distributed under the terms of the Creative Commons Attribution License (<http://creativecommons.org/licenses/by/2.0>), which permits unrestricted use, distribution, and reproduction in any medium, provided the original work is properly cited.

MACS

(a)

Estimate d based on high quality peaks



The Poisson distribution

$$P(X \geq x) = 1 - \sum_0^{x-1} \frac{\lambda^x e^{-\lambda}}{x!}$$

λ =expected # of reads within an interval of $2d$ bp

$$\lambda_{\text{local}} = \max(\lambda_{\text{BG}}, [\lambda_{1k}, \lambda_{5k}, \lambda_{10k}])$$

in R $P(X \geq 5 | \lambda = 0.001)$ is $1 - \text{sum}(\text{dpois}(0:4, 0.001))$

BayesPeak

BMC Bioinformatics



Research article

Open Access

BayesPeak: Bayesian analysis of ChIP-seq data

Christiana Spyrou*^{1,3}, Rory Stark³, Andy G Lynch⁴ and Simon Tavaré^{2,4}

Address: ¹Statistical Laboratory, Centre for Mathematical Sciences, Wilberforce Road, Cambridge, UK, ²DAMTP, Centre for Mathematical Sciences, Wilberforce Road, Cambridge, UK, ³Cancer Research UK, Cambridge Research Institute, Li Ka Shing Centre, Robinson Way, Cambridge UK and ⁴Department of Oncology, University of Cambridge, Li Ka Shing Centre, Robinson Way, Cambridge, UK

Email: Christiana Spyrou* - C.Spyrou@statslab.cam.ac.uk; Rory Stark - Rory.Stark@cancer.org.uk; Andy G Lynch - Andy.Lynch@cancer.org.uk; Simon Tavaré - st321@cam.ac.uk

* Corresponding author

Published: 21 September 2009

Received: 8 May 2009

BMC Bioinformatics 2009, **10**:299 doi:10.1186/1471-2105-10-299

Accepted: 21 September 2009

This article is available from: <http://www.biomedcentral.com/1471-2105/10/299>

© 2009 Spyrou et al; licensee BioMed Central Ltd.

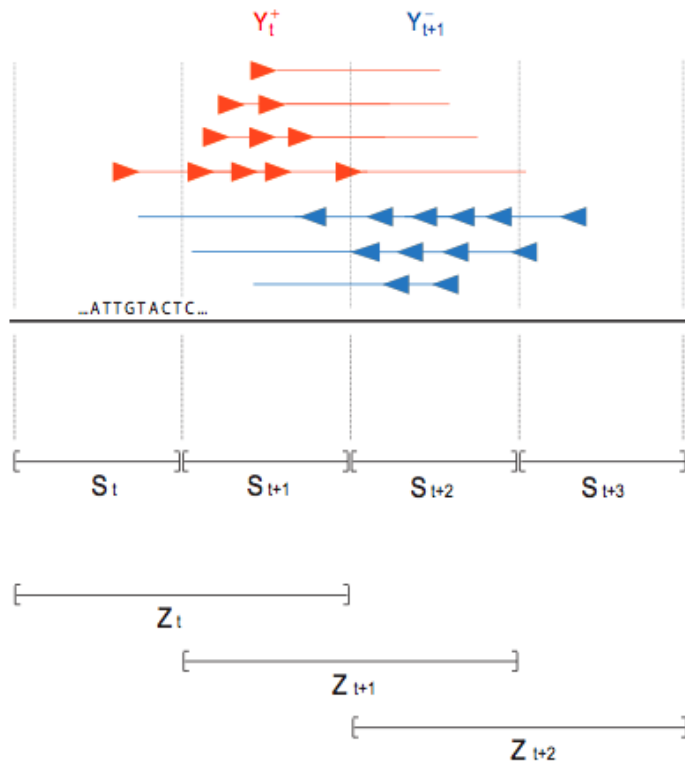
This is an Open Access article distributed under the terms of the Creative Commons Attribution License (<http://creativecommons.org/licenses/by/2.0>), which permits unrestricted use, distribution, and reproduction in any medium, provided the original work is properly cited.

Abstract

Background: High-throughput sequencing technology has become popular and widely used to study protein and DNA interactions. Chromatin immunoprecipitation, followed by sequencing of the resulting samples, produces large amounts of data that can be used to map genomic features such as transcription factor binding sites and histone modifications.

BayesPeak (Bayesian Hidden Markov Models)

Observed variable



$$Z_t = \begin{cases} 0 & \text{if } (S_t, S_{t+1}) = (0, 0) \\ 1 & \text{if } (S_t, S_{t+1}) = (0, 1) \\ 2 & \text{if } (S_t, S_{t+1}) = (1, 0) \\ 3 & \text{if } (S_t, S_{t+1}) = (1, 1) \end{cases}$$

The emission distributions of the model are

$$\begin{aligned} Y_t^+, Y_{t+1}^- | Z_t = 0 &\sim \text{Poisson}(\lambda_0 \gamma^{w_t}) \\ Y_t^+, Y_{t+1}^- | Z_t = 1, 2, 3 &\sim \text{Poisson}((\lambda_0 + \lambda_1) \gamma^{w_t}) \\ \lambda_0 &\sim \Gamma(\alpha_0, \beta_0) \\ \lambda_1 &\sim \Gamma(\alpha_1, \beta_1) \end{aligned}$$

Hidden states

Parameters estimated using
Bayesian treatment

Other peak finders

Table 1: Comparison of different peak-calling algorithms

Method	A	B	C	D	E	F	G
CSPF	control or IP only	read length no orientation	merge strands no shift	N	simple height criteria	ROC curve (empirically)	both
XSET	IP only	fragment length orientation	merge strands no shift	Y	simple height criteria	FDR estimate using Poisson distribution	both
Mikkelsen et al.	IP only	no orientation	no merge no shift	Y	p -values from permutations	no official FDR	both
MACS	control or IP only	fragment length orientation no duplicated reads	shift reads merge strands	N	Poisson p -values	FDR estimate by peaks in control:IP	both
QuEST	control	orientation	shift reads merge strands	N	kernel density estimation	FDR estimate by permutations of the control	better for TF
FindPeaks	IP only	fragment length orientation	no merge no shift	N	simple height criteria	FDR estimate by permutations of the IP	both
SISSR	control or IP only	fragment length orientation	no merge no shift	N	compares reads on different strands	FDR estimate by peaks in background:IP	better for TF
Kharchenko et al.	control	orientation	no merge no shift	N	Poisson distribution	FDR estimate by permutations of the control	better for TF
PeakSeq	control	fragment length orientation	merge strands	Y	sample normalisation Binomial distribution	FDR estimate, q - values (BH correction)	both
BayesPeak	control or IP only	fragment length orientation	no merge no shift	N	negative binomial distribution, Bayesian posterior probabilities	posterior enrichment probabilities	both

The methods shown are compared with respect to the following features:

A. whether they require a control sample (control) or whether they only use the ChIP sample (IP only)

B. whether they take into account the (average) length of the reads/fragments and their orientation

C. whether they take into account the different DNA strands or if they merge the reads, and whether the reads are shifted towards the 3' end

D. whether an externally estimated mappability file is used

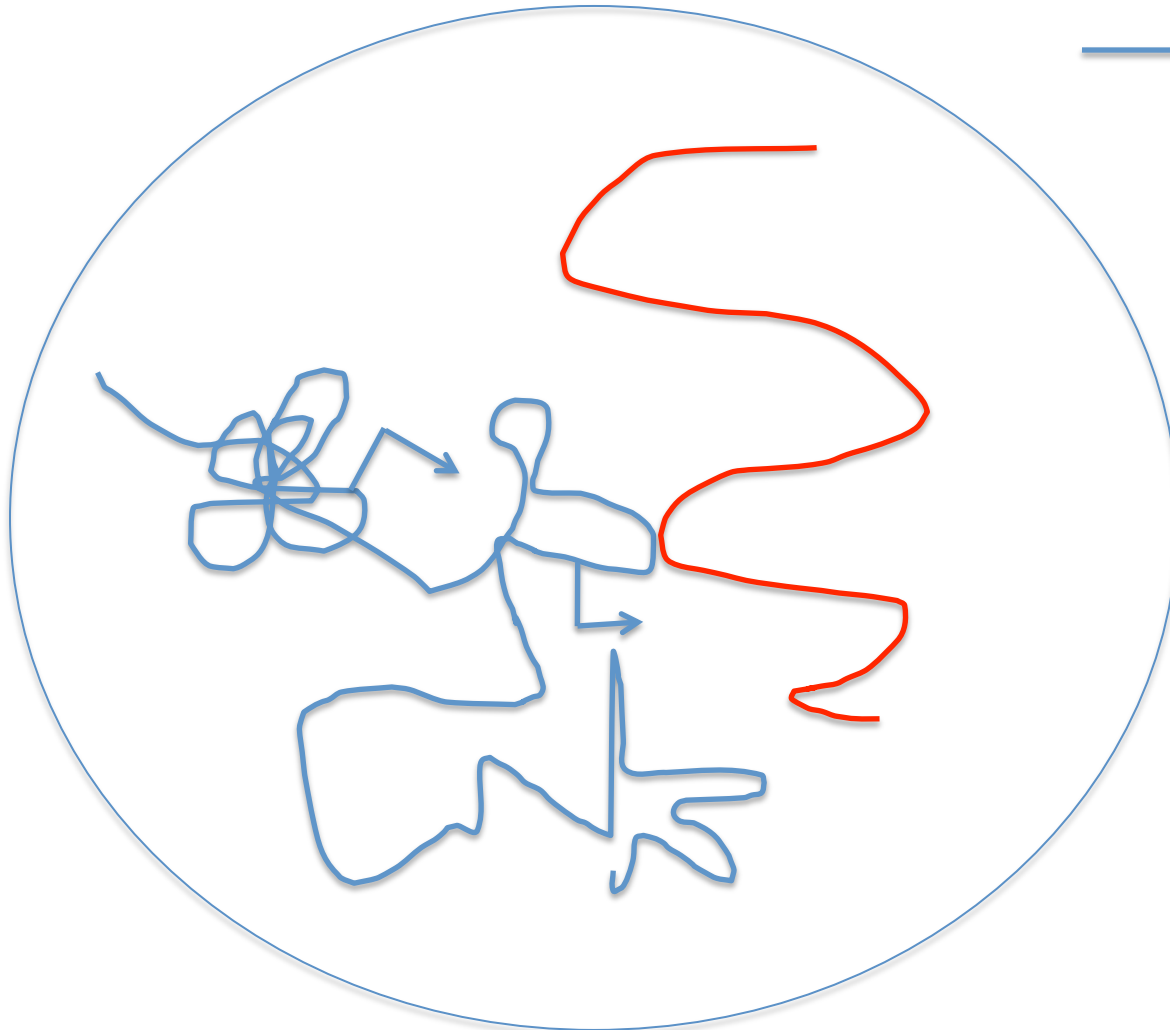
E. how the scores, on which the classifications are based, are estimated

F. whether/how any FDR or sensitivity/specificity estimates are calculated

G. whether or not the method is applicable to both transcription factor (TF) and histone mark data.

Mapping chromatin interactions using the Hi-C technique

The human genome is not linear



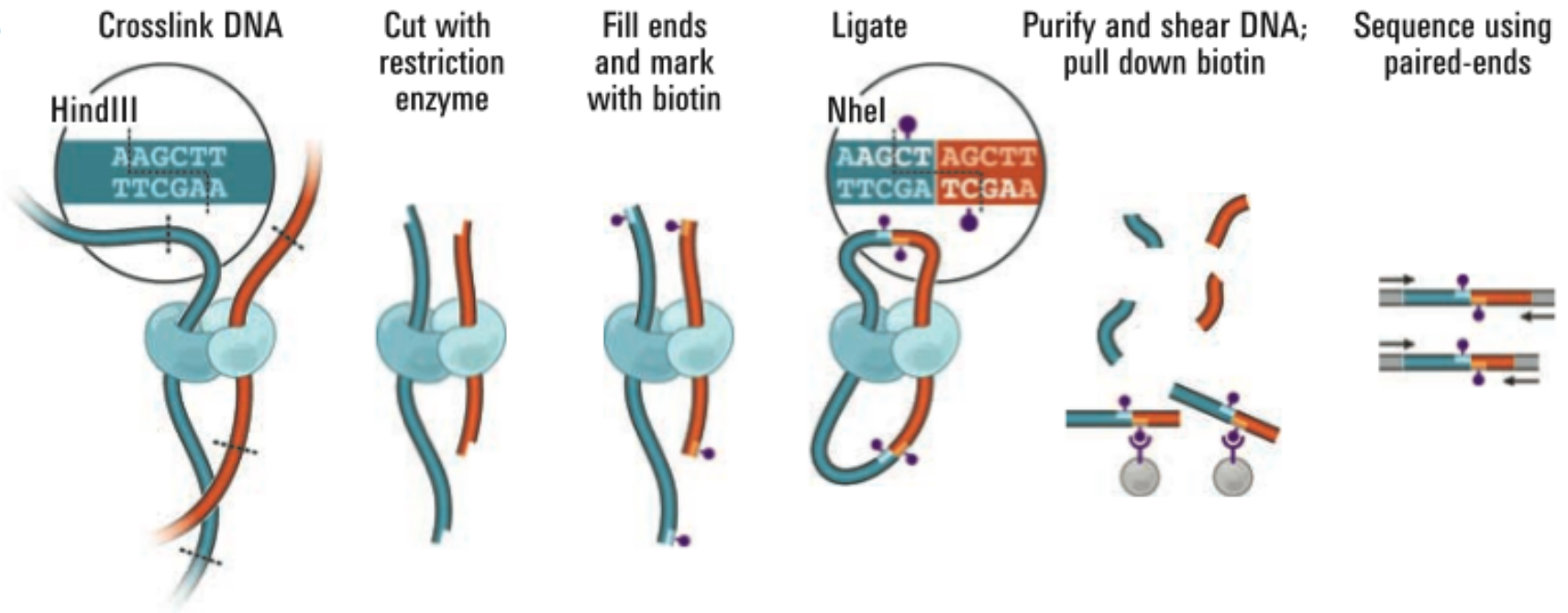
Terminology:
Intra-chromosomal interaction
Inter-chromosomal interaction
Interaction hub

How dynamic is the three dimensional architecture of the human genome ?

How does 3D localization impact gene expression ?

Is the 3D genome different in normal cells and cancer cells ?

Genome-scale mapping of chromatin interactions using HiC



Can a single (oncogenic) transcription factor induce global changes in chromatin structure ?

RESEARCH ARTICLE

Recurrent Fusion of *TMPRSS2* and ETS Transcription Factor Genes in Prostate Cancer

Scott A. Tomlins,¹ Daniel R. Rhodes,^{1,2} Sven Perner,^{7,9}
Saravana M. Dhanasekaran,¹ Rohit Mehra,¹ Xiao-Wei Sun,⁷
Sooryanarayana Varambally,^{1,6} Xuhong Cao,¹ Joelle Tchinda,⁷
Rainer Kuefer,¹⁰ Charles Lee,⁷ James E. Montie,^{3,5,6}
Rajal B. Shah,^{1,3,5,6} Kenneth J. Pienta,^{3,4,5,6} Mark A. Rubin,^{7,8}
Arul M. Chinnaiyan^{1,2,3,5,6*}

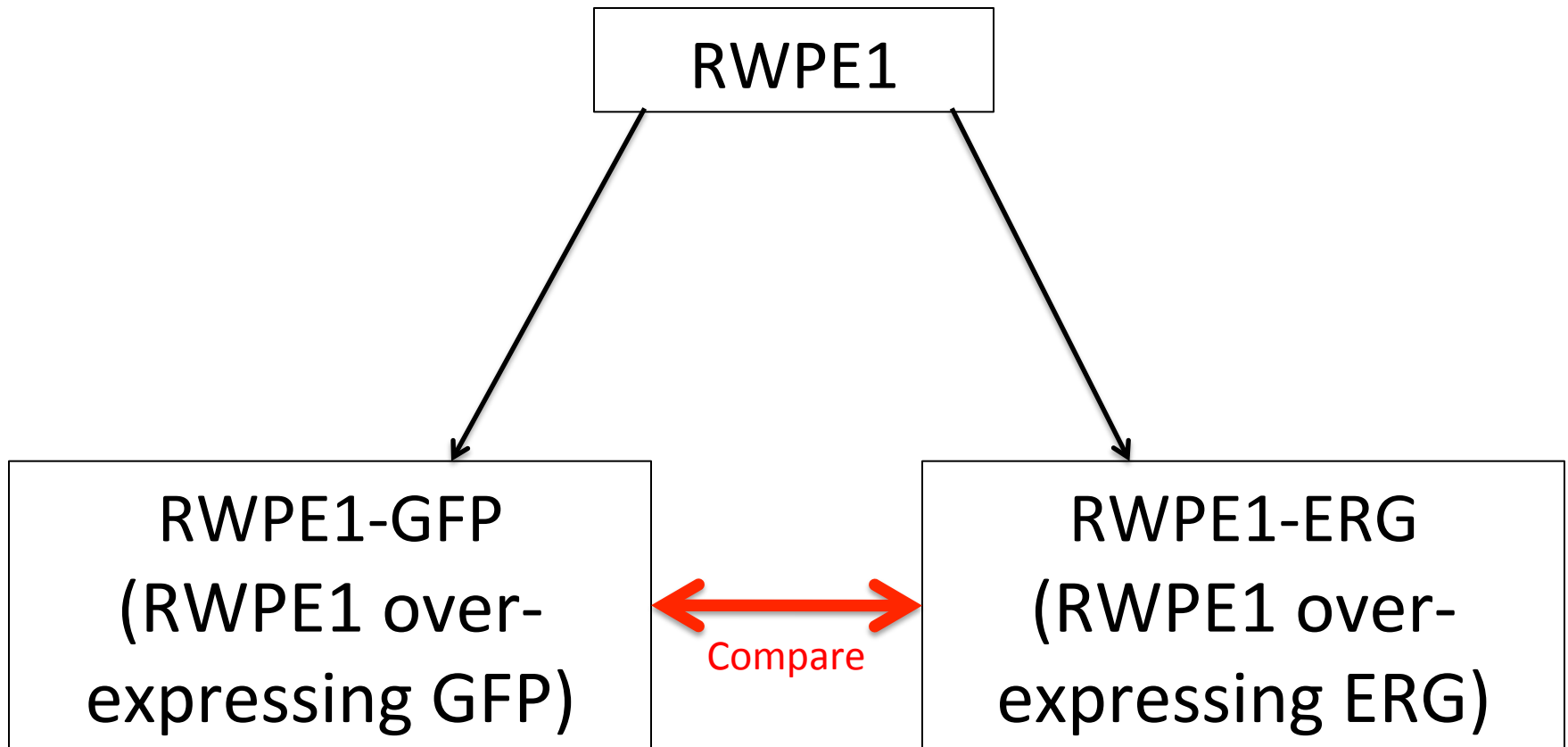
Recurrent chromosomal rearrangements have not been well characterized in common carcinomas. We used a bioinformatics approach to discover candidate oncogenic chromosomal aberrations on the basis of outlier gene expression. Two ETS transcription factors, *ERG* and *ETV1*, were identified as outliers in prostate cancer. We identified recurrent gene fusions of the 5' untranslated region of *TMPRSS2* to *ERG* or *ETV1* in prostate cancer tissues with outlier expression. By using fluorescence in situ hybridization, we dem-

(6). This karyotypic complexity is thought to reflect secondary genomic alterations acquired during tumor progression.

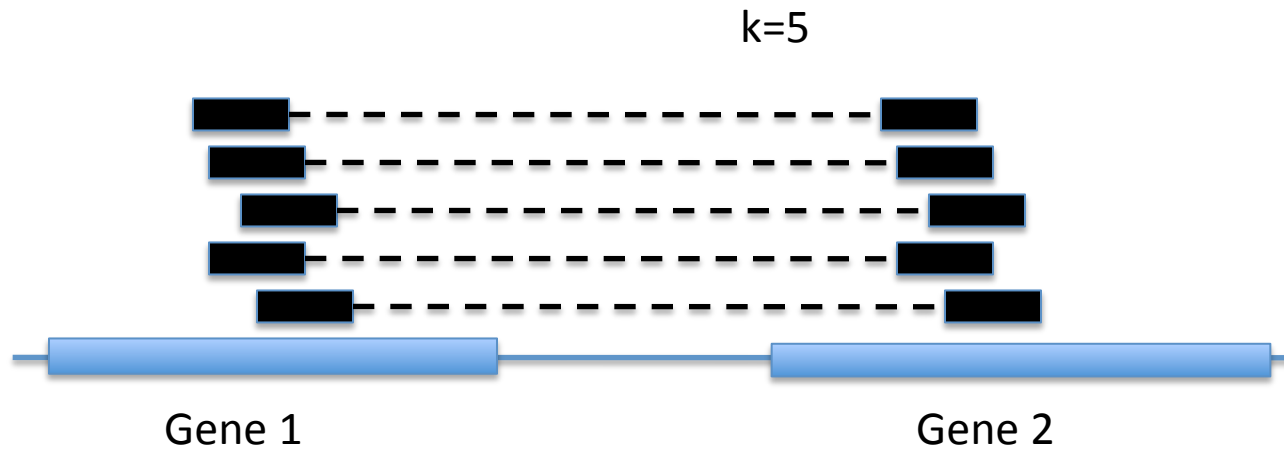
We hypothesized that rearrangements and high-level copy number changes that result in marked overexpression of an oncogene should be evident in DNA microarray data but not necessarily by traditional analytical approaches. In the majority of cancer types, heterogeneous patterns of oncogene activation have been observed; thus, traditional analytical methods that search for common activation of genes across a class of cancer samples (e.g., *t* test or signal-to-noise ratio) will fail to find such oncogene expression profiles. Instead, a method that searches for marked overexpression in a subset of cases is needed. Toward this end, we developed a method termed cancer outlier profile analysis (COPA). COPA seeks to accentuate and identify outlier profiles by applying a simple numerical transformation based on the median and median absolute deviation of a gene expression profile (7) (fig. S1A).

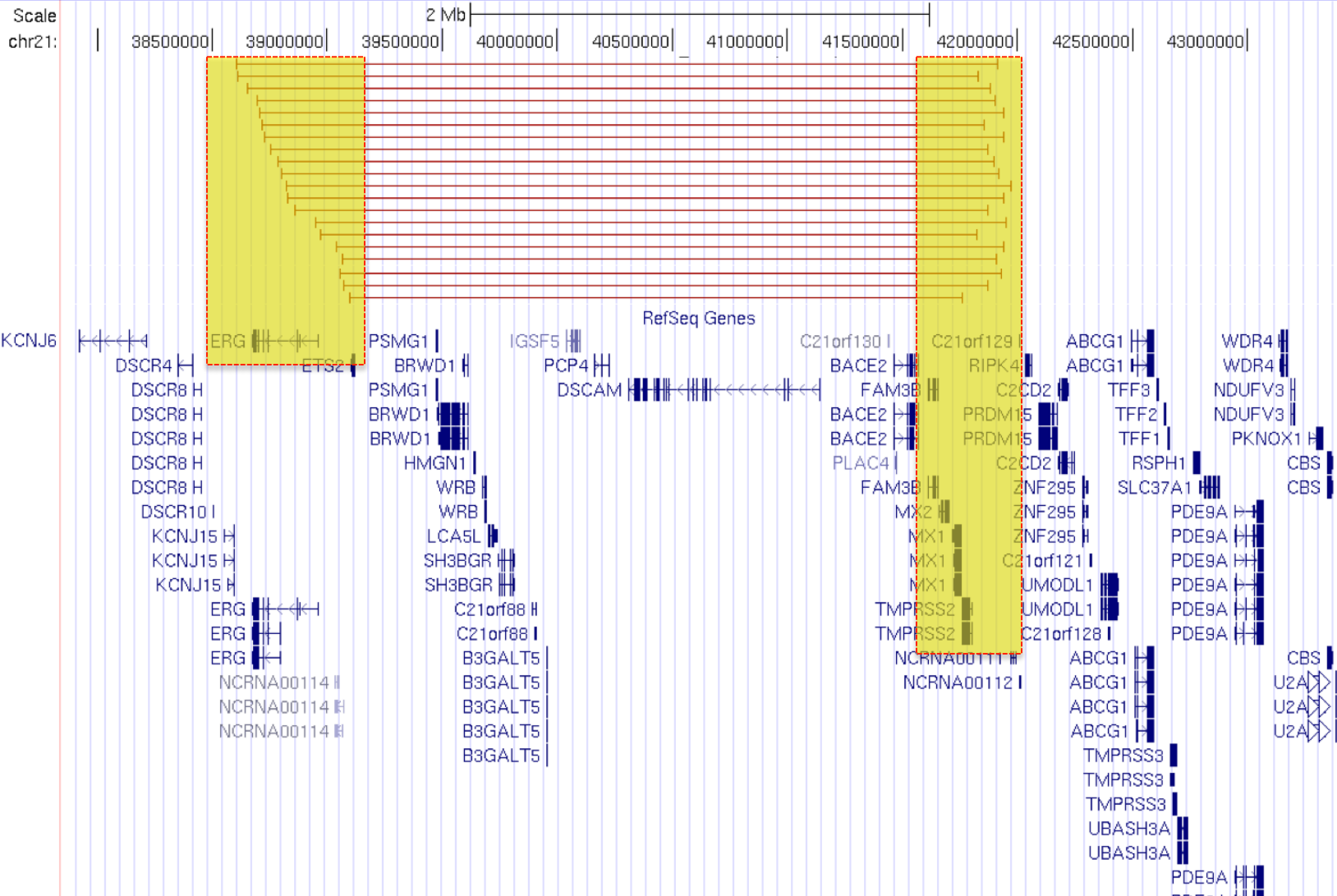
ERG is fused to *TMPRSS2* and over-expressed in > 50% of prostate tumors

Prostate epithelial lesion cell line (RWPE1)



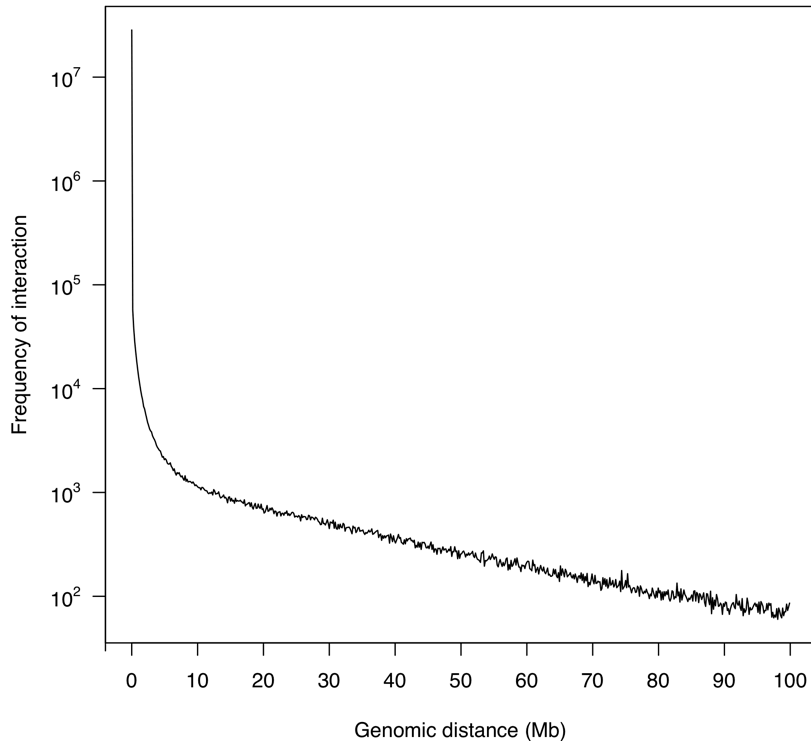
Quantifying proximity using HiC reads





Interaction frequency decreases with genomic distance

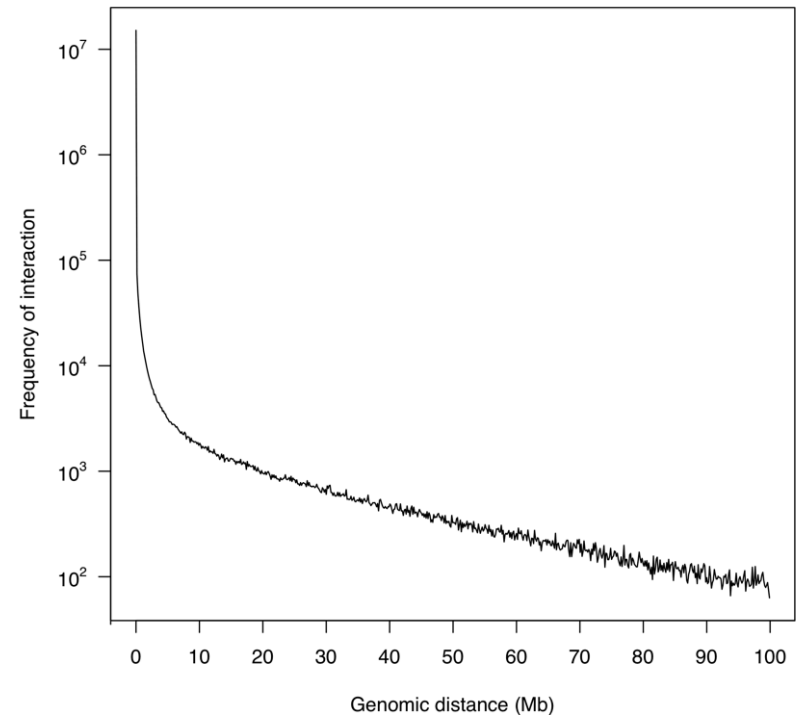
ERG



$$P_{\text{interaction}}(s) \sim s^{-1}$$

(500Kb-1Mb range)

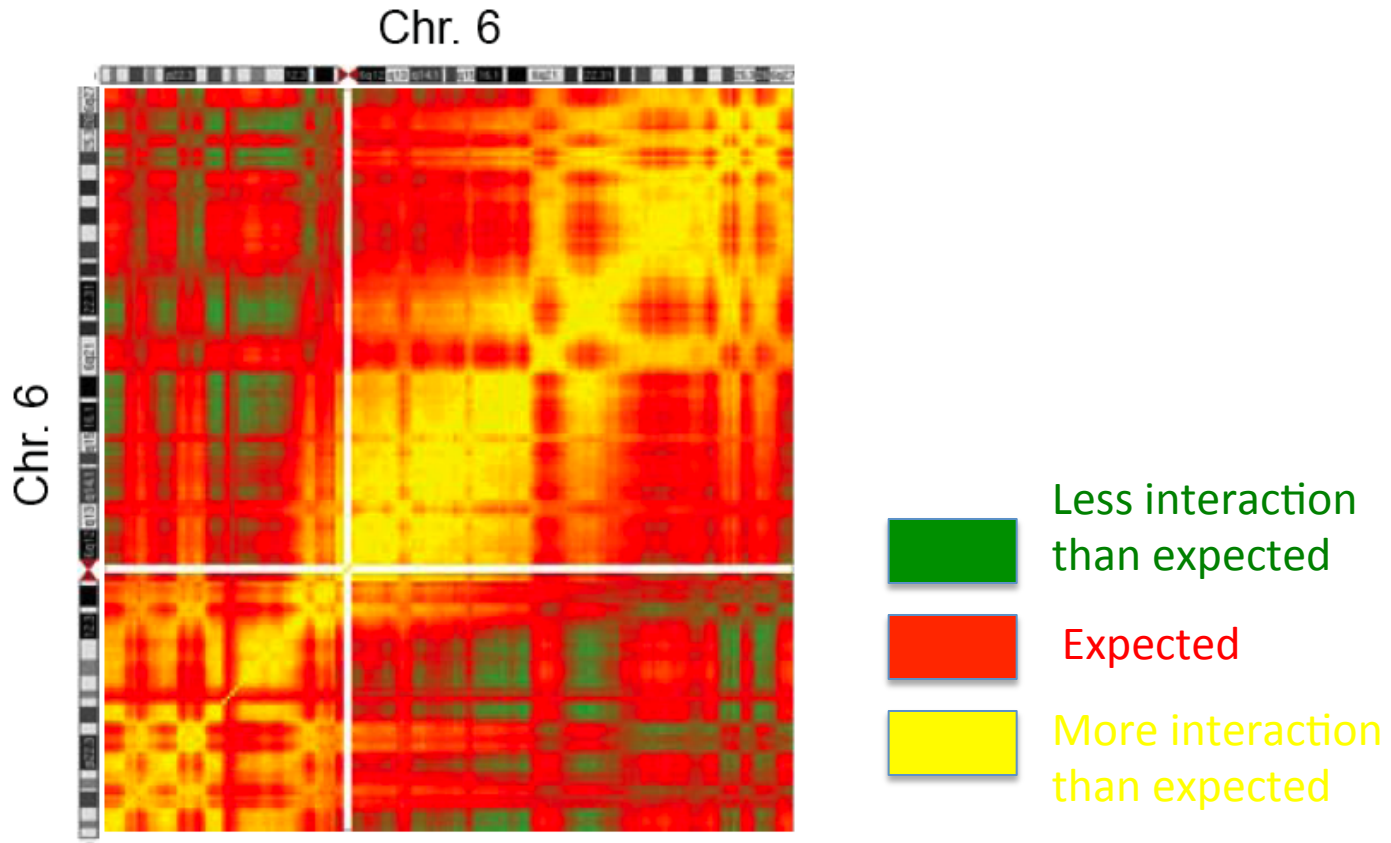
GFP



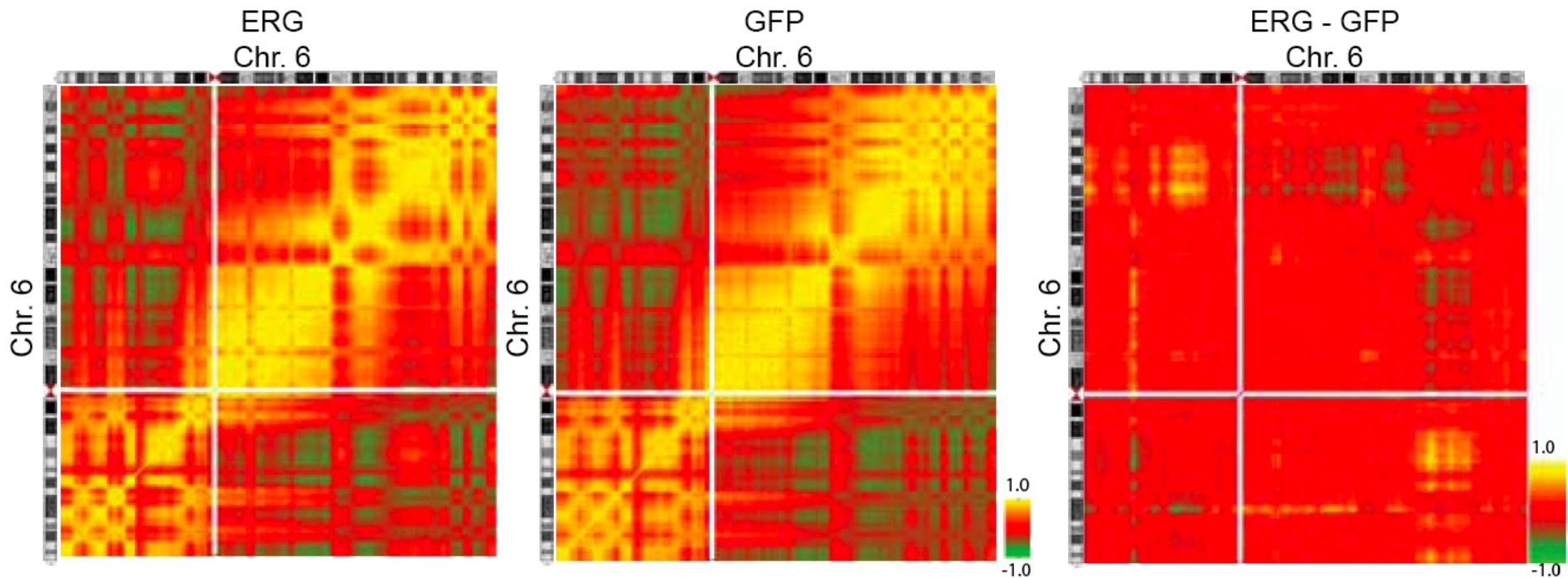
$$P_{\text{interaction}}(s) \sim s^{-1}$$

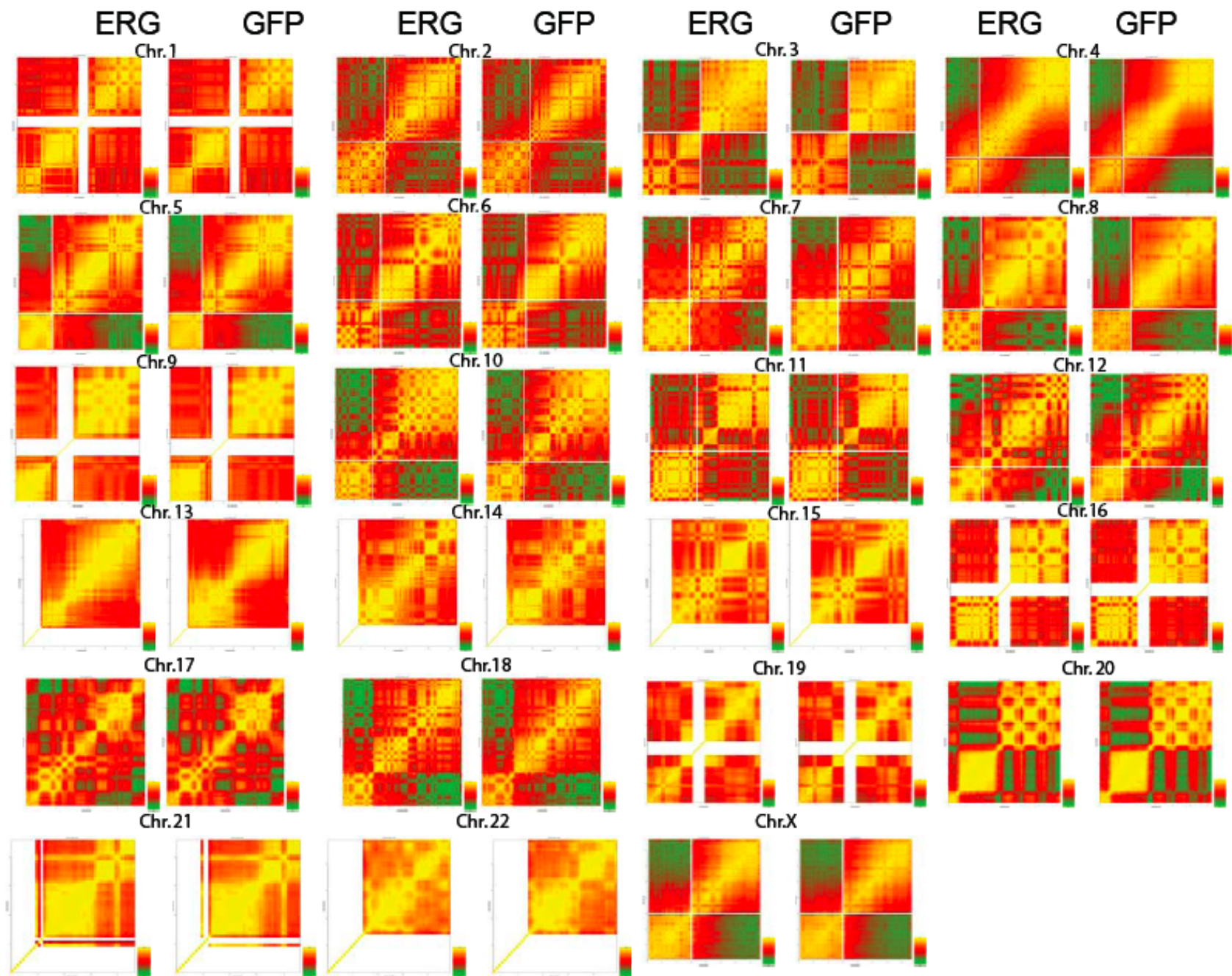
(500Kb-1Mb range)

Contact maps show domains of interactions



There are differences in interactions between ERG and GFP cells

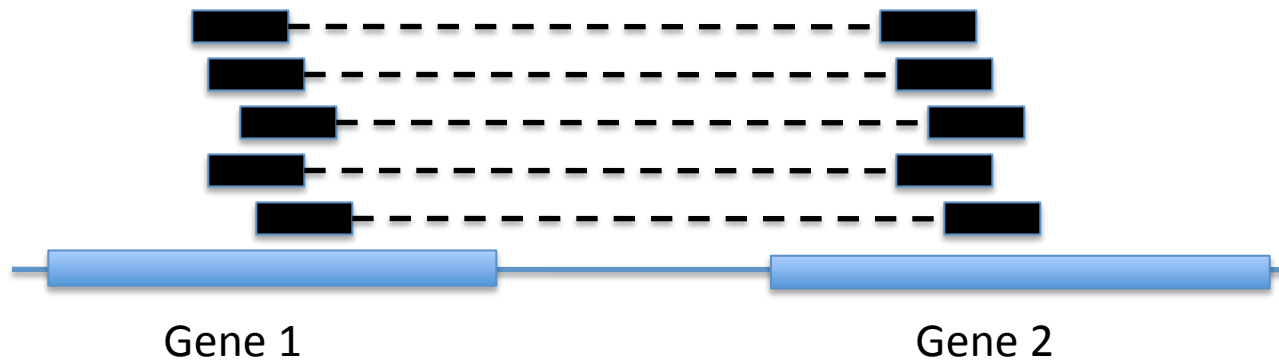




Fisher exact tests to quantify difference in interactions between GFP and ERG

GFP

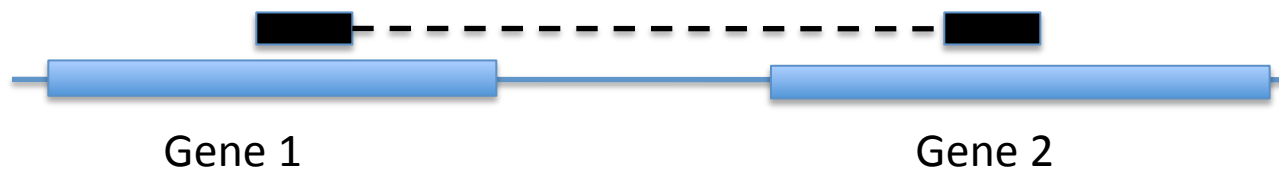
k=5



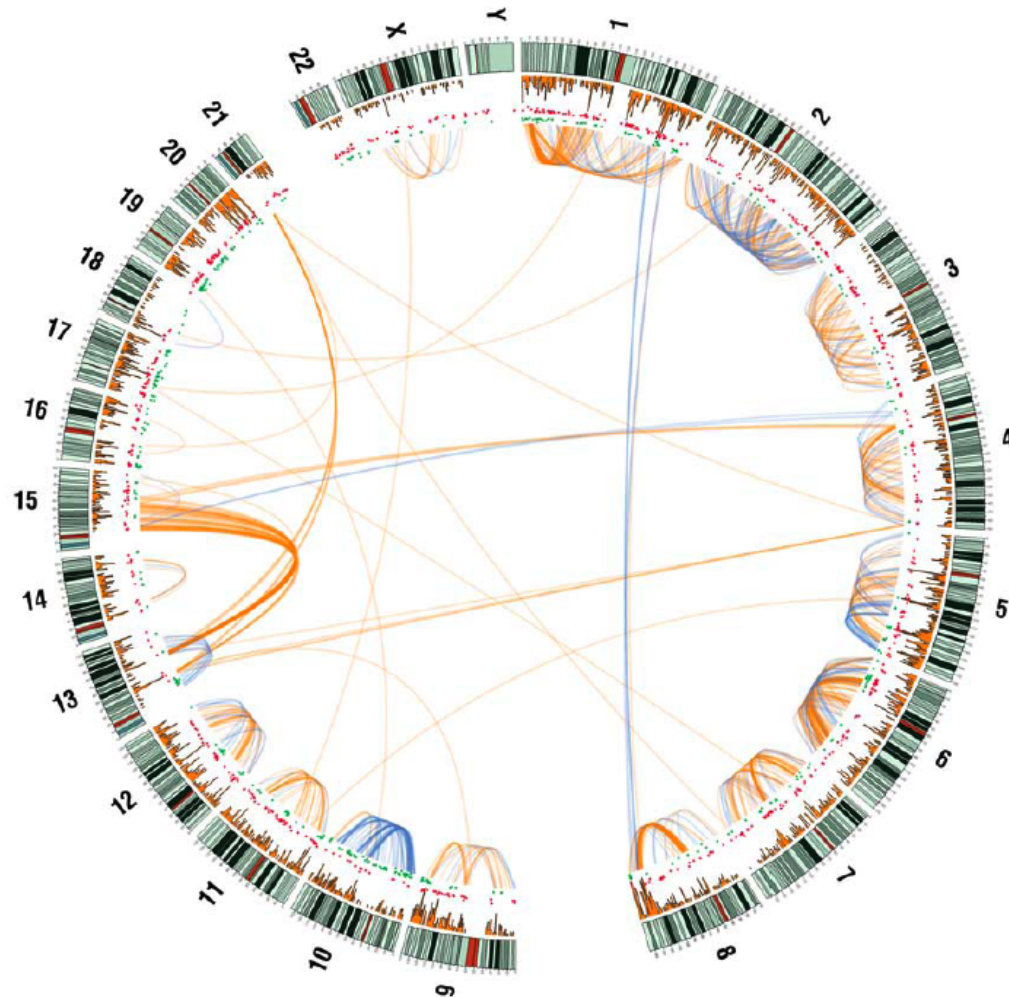
$$P(X = k) = \frac{\binom{m}{k} \binom{N-m}{n-k}}{\binom{N}{n}}$$

ERG

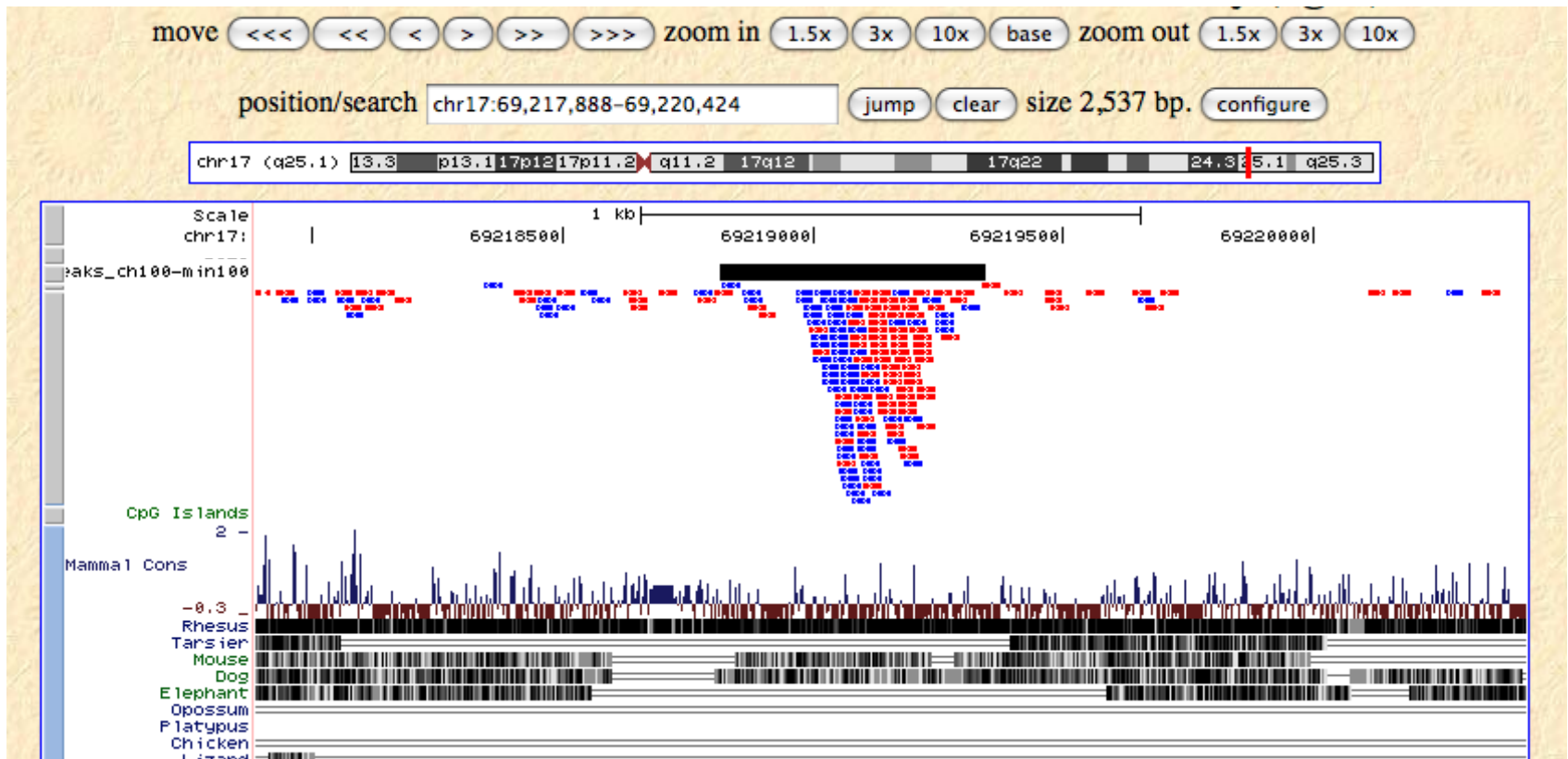
k=1



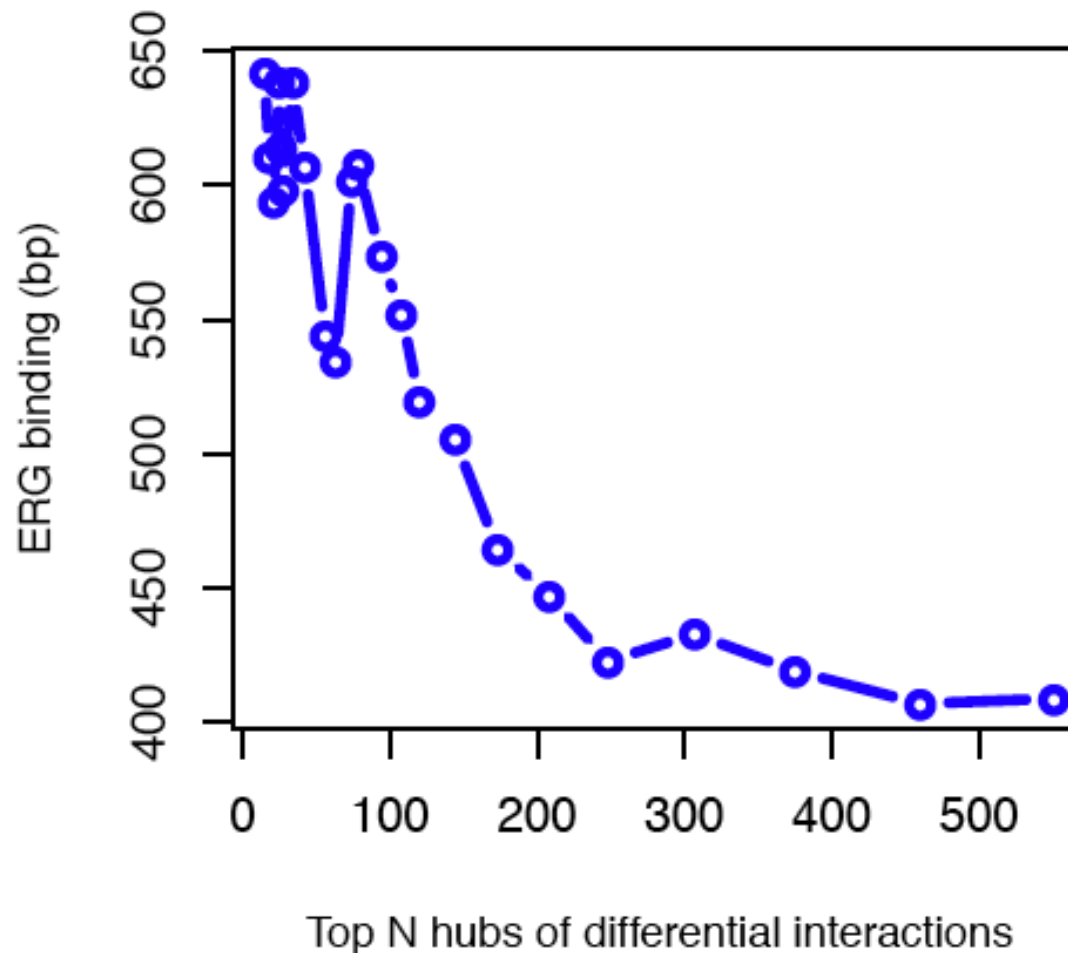
A graphical representation of all **gains** or **losses** of interaction in ERG cells vs GFP



ChIP-seq: ERG binds to >6,000 location in RWPE1-ERG cells



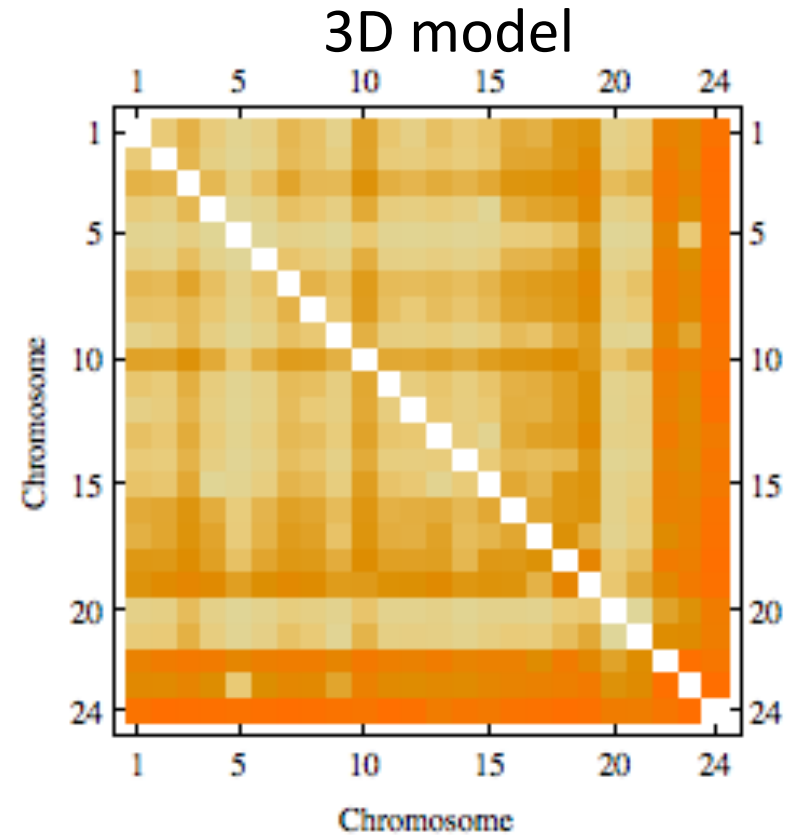
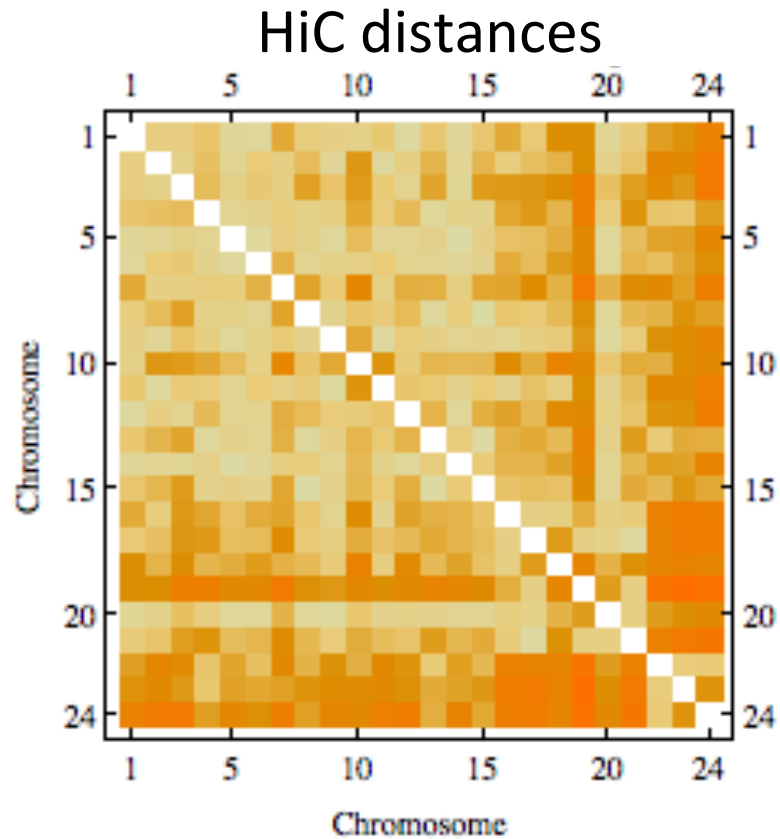
Loci/genes that **lose** or **gain** many interactions are more likely to be bound by ERG



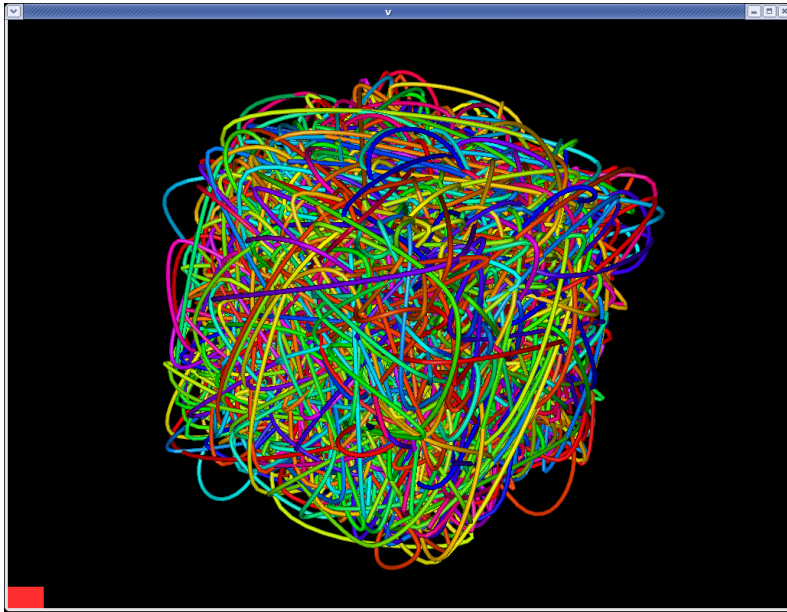
3D genome models

- Bin the genome into 1Mb blocks
- $D = 1 / k$ where k = number of reads “connecting” two blocks
- Start with random 3D topologies, use gradient descent algorithm to make 3D models that best recapitulate the HiC distances

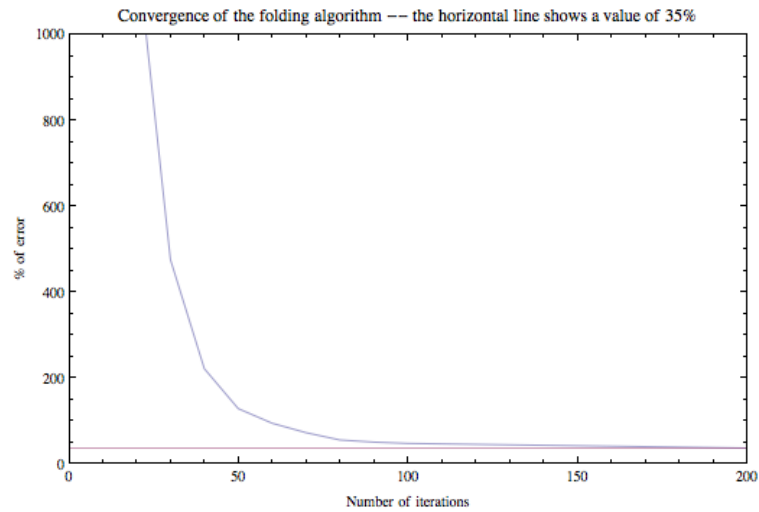
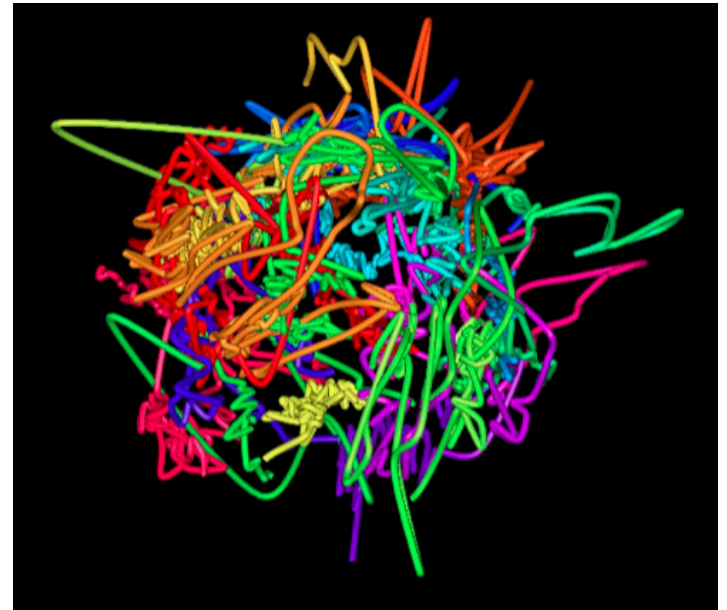
3D genome models

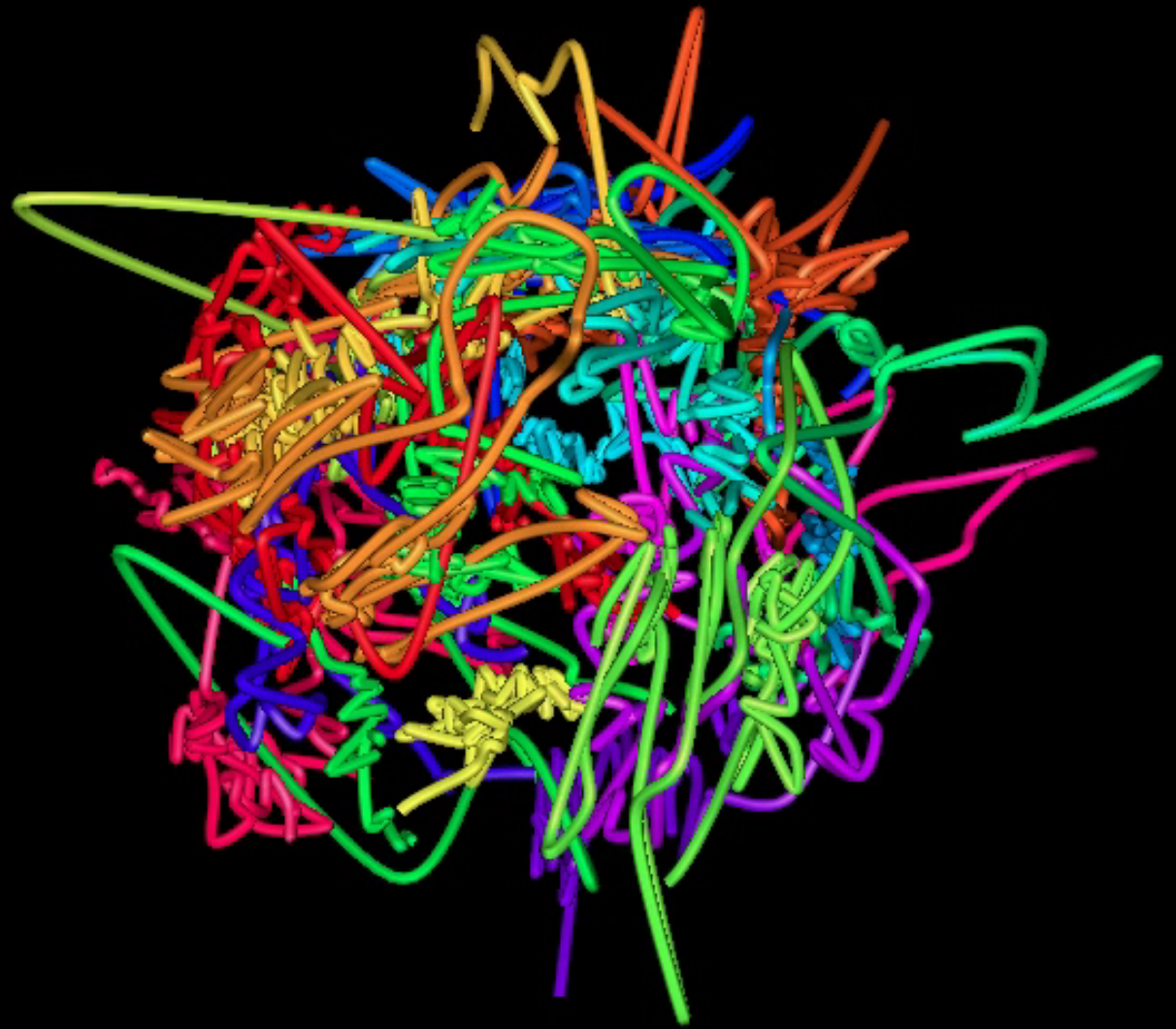


Initial random model



Final model





How does ERG over-expression change chromosome conformation ?

